GENDER AND THE GENOME
Volume 00, Number 00, 2017

DOI: 10.1089/gg.2017.0017

ORIGINAL ARTICLE

Sex-Specific Differences in Oxytocin Receptor Expression and Function for Parental Behavior

Mariela Mitre, PhD,[1–5,*] Thorsten M. Kranz, PhD,[1–5,*] Bianca J. Marlin, PhD,[1–4] Jennifer K. Schiavo, BA,[1–4] Hediye Erdjument-Bromage, PhD,[1,6] Xinying Zhang,[7] Jess Minder, BA,[1–4] Thomas A. Neubert, PhD,[1,6] Troy A. Hackett, PhD,[8] Moses V. Chao, PhD,[1,2,4,5] and Robert C. Froemke, PhD[1–4]

Abstract

Parental care is among the most profound behavior expressed by humans and other animals. Despite intense interest in understanding the biological basis of parental behaviors, it remains unknown how much of parenting is encoded by the genome and which abilities instead are learned or can be refined by experience. One critical factor at the intersection between innate behaviors and experience-dependent learning is oxytocin, a neurohormone important for maternal physiology and neuroplasticity. Oxytocin acts throughout the body and brain to promote prosocial and maternal behaviors and modulates synaptic transmission to affect neural circuit dynamics. Recently we developed specific antibodies to mouse oxytocin receptors, found that oxytocin receptors are left lateralized in female auditory cortex, and examined how oxytocin enables maternal behavior by sensitizing the cortex to infant distress sounds. In this study we compare oxytocin receptor expression and function in male and female mice. Receptor expression is higher in adult female left auditory cortex than in right auditory cortex or males. Developmental profiles and mRNA expression were comparable between males and females. Behaviorally, male and female mice began expressing parental behavior similarly after cohousing with experienced females; however, oxytocin enhanced parental behavior onset in females but not males. This suggests that left lateralization of oxytocin receptor expression in females provides a mechanism for accelerating maternal behavior onset, although male mice can also effectively co-parent after experience with infants. The sex-specific pattern of oxytocin receptor expression might genetically predispose female cortex to respond to infant cues, which both males and females can also rapidly learn.

Keywords: behavior, lateralization, mouse, oxytocin

Introduction

Oxytocin is a peptide hormone involved in many physiological processes and especially important for maternal behaviors and pair bond formation.[1–7] Oxytocin is primarily synthesized in the hypothalamic paraventricular nucleus (PVN) and supraoptic nucleus and secreted into the body from hypothalamic nerve terminals constituting the posterior pituitary.[6,8–12] Hypothalamic neurons also project and release oxytocin throughout the brain,[3,4,6,10–21] although it remains unclear how a peptide important for water homeostasis and milk ejection is also involved in regulation of neural circuit function and social cognition for parenting behavior. A long literature of studies in voles and other mammals indicate that the pattern of oxytocin receptor expression is an important factor related to social and parental behaviors,[2–5,16–32] but it has largely remained unclear which cells or synapses express oxytocin receptors and are directly modulated by oxytocin.

Thus it has been challenging to relate the physiological effects of oxytocin receptor signaling to behavioral consequences. This confounds attempts to understand and optimize if or how oxytocin might be used in humans to improve social behavior, including therapeutic treatments

[1]Skirball Institute for Biomolecular Medicine, [2]Neuroscience Institute, New York University School of Medicine, New York, New York.
Departments of [3]Otolaryngology, [4]Neuroscience and Physiology, [5]Cell Biology, Psychiatry, and [6]Biochemistry and Molecular Pharmacology, New York University School of Medicine, New York, New York.
[7]New York University, Shanghai, China.
[8]Department of Hearing and Speech Sciences, Vanderbilt Kennedy Center for Research on Human Development, Vanderbilt University School of Medicine, Nashville, Tennessee.
*These authors are co-first authors.

for psychiatric conditions such as autism spectrum disorders or postpartum depression.[6,33–38]

To understand how oxytocin influences parental behaviors—or social cognition more broadly—requires robust animal models of maternal and paternal interactions. A remarkable series of studies in rodents has demonstrated that oxytocin can enable or induce pair bond formation and maternal behavior, either when directly infused into the brain or systemically injected.[18,19,22,25] Parental behavior such as retrieval of isolated pups, nest building, and nursing are relatively straightforward to document and reliably expressed by experienced maternal mammals.

In contrast, paternal behavior in male rodents is less clear, with reports of infanticide or neglect unless males are mated, cohoused with experienced females, and/or have undergone physiological changes to steroid hormone or hypothalamic peptide systems, for example, cells expressing galanin or vasopressin.[39–47] Male mice and other mammals, including humans, express oxytocin receptors and experience heightened levels of plasma oxytocin during some social interactions.[6,16,48–52] However, it remains unclear whether there are important differences in the organization of the oxytocin system in females and males, and how oxytocin might be involved in establishing paternal behavior.

We recently generated new antibodies specific to the mouse oxytocin receptor, to determine where and when oxytocin receptors are expressed with increased precision and help understand the functional consequences of oxytocin receptor activation for synaptic transmission and neural signaling.[21] We showed that both endogenous oxytocin (released optogenetically) and exogenous oxytocin (either injected systemically or directly infused into left auditory cortex) could enable the initial expression of pup retrieval behavior. In pup-naive virgin female mice cohoused with an experienced dam and litters, oxytocin accelerated retrieval onset and increased the overall number of female virgins expressing this alloparenting behavior.[18]

In this study we now use these antibodies to compare the pattern of oxytocin receptor expression in males to females, throughout development and in adults. We also examine changes in gene expression and parental behavior after oxytocin supplements, contrasting sex-specific functional effects that might depend on differential receptor expression in males and females. We focus on the auditory cortex given the importance of this brain area for learning to recognize the behavioral significance of mouse pup isolation distress calls.[18]

Materials and Methods

All procedures were approved under NYU IACUC protocols. In this study we report results from a total of 134 female and 55 male C57BL/6 mice; of which 43 males and 23 females were not previously described in our past studies of oxytocin receptor expression and function.[18,21]

Immunohistochemistry

OXTR-2 antibodies were generated and validated as previously described.[18,21] For immunohistochemical analysis with light microscopy, wild-type or oxytocin receptor knockout C57BL/6 mice were anesthetized using intraperitoneal (IP) injection (0.1 mL per 10 g) of a ketamine–xylazine mixture containing 15 mg/mL ketamine and 5 mg/mL xylazine in 0.9% sodium chloride solution. Mice were perfused intracardially with a solution of heparin (1000 U/mL) and PBS to prevent clotting, followed by 40 mL per mouse of freshly prepared 4% paraformaldehyde in 10 mM phosphate buffer. The brains were carefully removed and post-fixed in 4% paraformaldehyde for 2 h at 4°C and then cryoprotected overnight in 30% sucrose at 4°C. The brains were then embedded in a cryoprotectant medium (Tissue-Tek, Optimum Cutting Temperature medium, VWR) and stored at −80°C until sectioned. Coronal 16 μm sections were cut on a cryostat and collected on Superfrost Plus glass slides (Fisher Scientific).

Sections were washed in PBS and blocked for 2–3 h at room temperature in PBS containing 0.2% v/v Triton X-100 and 5% v/v normal donkey serum. The blocking solution was aspirated, and the sections were incubated with oxytocin receptor primary antibody diluted in block to a concentration of 1 μg/mL. Sections were incubated for 2 days at 4°C in a moist chamber. Sections were washed with PBS (3×15 min at room temperature) in a staining jar and incubated for 1–2 h at room temperature in Alexa Fluor-conjugated secondary antibodies diluted 1:500 in PBS. Any unbound secondary antibody was washed with PBS (3×15 min at room temperature), and sections were incubated for 15 min at room temperature with a DAPI solution (1:10,000 stock diluted in PBS) for nuclear staining.

After a final rinse, the slides were coverslipped using Fluoromount G (Southern Biotechnology Associates, Inc.). The brains of wild-type and knockout animals were processed together to minimize any confounding factors, and parallel sections from knockout animals served as controls. As a control, omission of primary antibody eliminated immunofluorescent labeling from that channel.

Slides were examined and imaged using a Carl Zeiss LSM 700 confocal microscope with four solid-state lasers (405/444, 488, 555, 639 nm) and appropriate filter sets. The distribution and number of immunoreactive cells in each section were determined by taking images of wild-type and knockout sections under the same laser power output, pinhole aperture, and gain. Images were collected and saved for manual counts by two to five independent blinded observers. Maximum intensity projections of image stacks are shown, each representing at least six to eight distinct optical planes.

Next-generation sequencing of total RNA

Frozen brains from six animals in each age group (three male, three female) were sectioned in the coronal plane (rostral to caudal) on a sliding microtome and viewed through a surgical microscope.[21,53] As areas targeted for sampling became visible, they were extracted using a sterile tissue punch or curette of a size appropriate to the brain region. Samples of auditory cortex were obtained using a 0.5 mm diameter punch, with the ventral edge beginning ~1 mm dorsal to the rhinal fissure. Samples of medial geniculate body (MGB) were harvested with a curette after using a microdissecting scalpel to circumscribe its perimeter, and the microdissection procedure was designed to exclude the lateral geniculate nucleus and adjoining nuclei dorsal, medial, and ventral to the MGB. The extreme rostral and caudal poles of the MGB were largely excluded from these

samples. Punches from homologous areas of both hemispheres were combined in sterile tube containing 400 μL of TRIzol, homogenized for 45 s using a mechanized sterile pestle, flash frozen on dry ice, and then stored at −80°C.

For each TRIzol lysate, 100 μL of Reagent Grade Chloroform (Fisher Scientific; S25248) were added. Samples were centrifuged for 3 min on a desktop centrifuge to fractionate the aqueous and organic layers. After centrifugation, the resulting aqueous layer was carefully removed and transferred to 2.0 mL Sarstedt tubes (Sarstedt; 72.694) were run on the QIAsymphony using the QIAsymphony RNA Kit (Qiagen; 931636) and protocol RNA_CT_400_V7, which incorporates DNAse treatment. Before each run, the desk was uv-irradiated using the programmed cycle. The resulting RNA was eluted to 100 μL of RNase free water and stored at −80°C in 2.0 mL Sarstedt tubes until use. Samples were initially quantitated using a Qubit RNA assay. Additional analyses of purity and quantitation of total RNA were performed using a NanoDrop spectrophotometer (Thermo Scientific) and Agilent RNA 6000 Pico chip (Agilent) according to the manufacturer's protocol using reagents, chips, and ladder provided in the kit.

RNA-seq was performed by the Vanderbilt Technologies for Advanced Genomics core (VANTAGE) as previously described.[21,53] Total RNA was isolated with the Aurum Total RNA Mini Kit. All samples were quantified on the Qubit RNA assay. RNA quality was verified using an Agilent Bioanalyzer. RNA-seq data were obtained by first using the Ribo-Zero Magnetic Gold Kit (Human/Mouse/Rat) (Epicentre) to perform ribosomal reduction on 1 μg total RNA following manufacturer's protocol. After ribosomal RNA (rRNA) depletion, samples were purified using the Agencourt RNAClean XP Kit (Beckman Coulter) according to the Epicentre protocol specifications. After purification, samples were eluted in 11 μL RNase-free water.

Next, 1 μL ribosomal depleted samples were run on the Agilent RNA 6000 Pico Chip to confirm rRNA removal. After confirmation of rRNA removal, 8.5 μL rRNA-depleted sample was input into the Illumina TruSeq Stranded RNA Sample Preparation Kit (Illumina) for library preparation. Libraries were multiplexed six per lane and sequenced on the HiSeq 2500 to obtain at least 30 million paired end (2 × 50 bp) reads per sample.

RNA-seq data went through multiple stages of quality control as previously described.[21] Normalized read counts were averaged over all samples for each age (P7, P14, P21, adult) and brain region (auditory cortex, auditory thalamus). ANOVA with Tukey *post hoc* testing was used to screen for significant differences in expression between ages for each area and gene.

Mass spectrometry

Dams and male C57BL/6 mice between 2–4 months of age were used for injection of oxytocin and saline ($N = 12$ mice total, 3 of each sex for each condition). For both sexes, the left auditory cortex was injected with 10 μM oxytocin and the right auditory cortex with 0.9% saline as vehicle control, under general anesthesia with 2% isoflurane. The injection volume for oxytocin and the vehicle was 1 μL over a period of 15 min (66 nL/min), respectively. After a total incubation time of 30 min, animals were decapitated, and the brain was extracted and flash frozen in liquid-nitrogen cooled isopentane in OCT and stored overnight at −80°C. Brains were sectioned using a cryostat. Sections at a thickness of 10 μM encompassing the auditory cortices on both hemispheres were mounted on glass slides with a polyethylene naphthalate membrane (PEN) (26 × 76 mm; Leica) and stored at −80°C.

Laser capture microdissection was performed using a LMD6500 microscope (Leica). Oxytocin, as well as vehicle injected auditory cortices, was collected separately in 0.5 mL PCR tubes. Protein extraction was performed using a RIPA buffer (1% (v/v) Triton X-100, 1% (v/v) SDS, 50 mM Tris-HCL pH 7.4, 500 mM NaCL, 1 mM EDTA) and 10 × aspiration using a U-100 Insulin Syringe (28G1/2, Becton Dickinson) for each sample. The samples were centrifuged at 16,900 *g* to remove cellular debris and PEN particles. Samples were denatured using 4 × Laemmli buffer (250 mM Tris-HCL pH 6.8), 8% SDS, 40% glycerol, 8% beta-Mercaptoethanol, and 0.02% bromophenol blue (Boston BioProducts) and run on 12% SDS-PAGE for subsequent mass spectrometry analysis.

Approximately 20–50 μg of each sample was concentrated by running briefly on 15% SDS/PAGE gels. Gels were washed 3 × in ddH2O for 15 min each and visualized by staining overnight with GelCode® Coomassie blue reagent (Pierce). The bands were excised from each gel, cut into slices, and reduced with DTT and alkylated with iodoacetamide. In-gel digestion was performed using mass spectrometry grade trypsin (Trypsin Gold; Promega, Madison, WI) at 5 ng/μL of 50 mM NH_4HCO_3 digest buffer. The resulting peptides were desalted using Sep-Pak tC18 1 cc Vac Cartridge (Waters, #WAT03820).

Tandem mass tag (TMT) labeling and the remaining proteomics protocol were carried out as previously described[54] with some modifications. Peptides were resuspended in 18 μL acetonitrile, and 262 μL of 0.2 M HEPES buffer pH 8.5 were added to each. TMT10plex amine reactive reagents (5 mg per vial) (Thermo Fisher Scientific) were resuspended in 1024 μL of anhydrous acetonitrile, and 24 μL of each reagent were added to each sample (TMT label:peptide [w/w] = 6:1) and mixed briefly on a vortexer. The mixture was incubated at room temperature for 1 h, quenched by the addition of 25 μL of 5% hydroxylamine for 15 min, and then acidified by the addition of 30 μL 10% formic acid. A small aliquot from each reaction was desalted on a Stage Tip manually packed with Empore C18 High Performance Extraction Disks (3 M; St. Paul, MN) and eluted peptide solutions partially dried under vacuum then analyzed by LC-MS/MS with a Q Exactive High Field Orbitrap mass spectrometer.[55] The data were searched in MaxQuant using its corresponding TMT label as variable modifications on N-terminus and lysine. The percentage of peptides with either N-terminal or lysine TMT labels was calculated, representing the labeling efficiency in each channel. To ensure that equal amounts of labeled peptides from each channel were mixed together, a two-step mixing strategy was used; in the first step, a small (∼5 μL) and identical volume of peptides from each channel was mixed and analyzed, and the value of the median ratio (defined by the median of the ratios of all peptide intensities of one channel over their corresponding peptide average intensities of all channels) for each channel was determined as the correction factor. In the second step,

the 7-plex mixed channels were prepared by adjusting their volume using the correction factors. In this way, a median ratio ranging from 0.9 to 1.1 was achieved. The mixture of reaction products from seven TMT channels was desalted on a Sep-Pak tC18 1 cc Vac Cartridge. Eluted peptides were dried and stored at −20°C. We prepared one 7-plex mix of peptides from two female mice and one male mouse and a second one that contained peptides from two male mice and one female mouse, each contributing right and left side of brain samples, annotated as 7-plex 1 and 7-plex 2, respectively. The seventh TMT channel in each mix was used as the reference channel consisting of a pool of all peptide samples.

TMT-labeled peptides were dissolved in 90% acetonitrile with 0.1% TFA. The TMT peptide mix was briefly centrifuged and injected on the HILIC column composed of TSK gel amide-80, 4.6 mm ID × 25 cm long, with 5 μm beads from TOSOH Bioscience, LLC. Peptides were eluted over a 65 min HPLC gradient with 300 μL flow rate. Peptides were collected every 4 min. Approximately 16 fractions were generated; 10% of each fraction was analyzed for quantitative analysis of the total proteome, and the remaining material was subjected to phosphopeptide enrichment step using Titanium dioxide chromatographic media (TiO2 beads; GL Sciences, Inc., Japan) as previously described.[54]

Online chromatography was performed with a Thermo Easy nLC 1000 UPLC system (Thermo Fisher Scientific) coupled online to a Q Exactive HF with a NanoFlex source (Thermo Fisher Scientific). Analytical columns (~30 cm long and 75 μm inner diameter) were packed in-house with ReproSil-Pur C18-AQ 3 μM reversed-phase resin (Dr. Maisch GmbH, Ammerbuch-Entringen, Germany).

The analytical column was placed in a column heater (Sonation GmbH, Biberach, Germany) set to a temperature of 45°C. Peptide mixtures were loaded onto the analytical column with buffer A (0.1% formic acid) at a maximum back pressure of 300 bar; peptides eluted with a 2-step gradient of 3% to 40% buffer B (100% ACN and 0.1% formic acid) in 180 min and 40% to 90% B in 20 min, at a flow rate of 250 nL/min over 200 min using a 1D online LC-MS2 data-dependent analysis method as follows: mass spectrometry data were acquired using a data-dependent top-10 method, dynamically choosing the most abundant not-yet-sequenced precursor ions from the survey scans (300–1750 Th).

Peptide fragmentation was performed using higher energy collisional dissociation with a target value of 1×10^5 ions determined with predictive automatic gain control. Isolation of precursors was performed with a window of 1 Th. Survey scans were acquired at a resolution of 120,000 at *m/z* 200. Resolution for HCD spectra was set to 60,000 at *m/z* 200 with a maximum ion injection time of 128 ms. The normalized collision energy was 35. The ''underfill ratio,'' specifying the minimum percentage of the target ion value likely to be reached at the maximum fill time, was defined as 0.1%. We excluded precursor ions with single, unassigned, or seven and higher charge states from fragmentation selection. Dynamic exclusion time was set at 30 s.

All data were analyzed with the MaxQuant proteomics data analysis workflow (version 1.6.0.1) with the Andromeda search engine.[56,57] The type of LC-MS run was set to ''Reporter ion MS2'' with ''10plex TMT'' as isobaric labels for Q Exactive MS2 data. Reporter ion mass tolerance was set to 0.01 Da, and the false discovery rate set to 1% for protein, peptide spectrum match, and site decoy fraction levels. Peptides were required to have a minimum length of eight amino acids and a maximum mass of 4600 Da. MaxQuant was used to score fragmentation scans for identification based on a search with an allowed mass deviation of the precursor ion of up to 4.5 ppm after time-dependent mass calibration. The allowed fragment mass deviation was 20 ppm. MS2 spectra were used by Andromeda to search the UniProt mouse database (16,729 entries).

Enzyme specificity was set as C-terminal to arginine and lysine, and a maximum of two missed cleavages was allowed. Carbamidomethylation of cysteine was set as a fixed modification, and N-terminal protein acetylation, deamidated (N, Q), and oxidation (M) were set as variable modifications. The reporter ion intensities were defined as intensities multiplied by injection time (to obtain the total signal) for each isobaric labeling channel summed over all MS/MS spectra matching to the protein group as previously validated.[57] Following MaxQuant analysis, the protein and peptide .txt files were imported into Perseus (version 1.6.0.2) software, which was used for the statistical analysis of all the proteins identified. The basic statistics used for significance analysis was the moderated *t*-statistics.[58] Benjamini–Hochberg correction was used to calculate the adjusted *p*-values.

Parental behavior

Two- to four-month-old C57BL/6 pup-naive virgin males, pup-naive virgin females, and dams were used for cohousing and analysis of pup retrieval and nest building. Male mice were raised with male littermates and had normal social interactions.[43–45] Male and female mice were bred on-site and weaned at P10, then housed in a separate environment not containing any dams or pups before cohousing. Virgin mice (either one male or one female) were then cohoused with a dam and litters ranging from P0-10. Dams were initially prescreened to ensure that they retrieved pups; ~1% of dams did not retrieve pups, and these animals were not used for cohousing. Naive virgins were initially prescreened for retrieval or pup mauling before cohousing; <30% of naive female virgins retrieved at least one pup or mauled pups during prescreening, while none of the males retrieved pups and only one male mauled pups before cohousing. These animals were excluded from subsequent behavioral studies.

Pup retrieval testing was performed as before,[18] in a similar manner for cohoused males or females. Testing included two parts: a habituation period and ~10 retrieval trials per testing session. During the habituation period, the animal was exposed to a novel behavioral arena (38 × 30 × 15 cm) with bedding and cotton balls for nest material. After 5–20 min (20–30 min on first testing session per animal), several pups from the cohousing home cage were introduced into the arena and placed in one corner together with cotton balls as a nest. In each retrieval trial, one pup was removed from the nest and placed in a different corner. Each trial lasted for 2 min and time to retrieval scored; if the animal did not retrieve after 2 min, the pup was put back in the nest, and another trial was initiated with a new pup. After ten trials were completed, the adult male or

female was injected IP with oxytocin (20–50 μM in saline) or saline alone at a volume of 0.3 mL per injection; animals were given 5–10 min to recover and retested for another 10 trials. Animals were then placed with the pups back in to the cage to continue cohousing.

Retrieval testing was performed at 1 h, 3 h, 6 h, 12 h, 24 h (1 day), 36 h, 48 h (2 days), 72 h (3 days), 96 h (4 days), 120 h (5 days), and 144 h (7 days). Animals in the oxytocin group received IP injections of oxytocin at each of these testing timepoints; animals in the saline group received IP injections of saline at each testing timepoint. We used an ultrasonic microphone (Avisoft) to verify that isolated pups vocalized during testing. Nest building by males was also monitored during each entire testing session. We defined nest building as animals biting and bringing the cotton balls near the pups as nesting material. Power analysis was performed to determine sample size for statistical significance with a power of β:0.7; these studies required at least six animals. Fisher's two-tailed exact test was used for comparing numbers of animals retrieving in each group as these data were binomial.

Results

Oxytocin receptor expression in left auditory cortex is higher in females than males

We first asked how oxytocin receptor expression differs between male and female mouse auditory cortex. Auditory cortical activity is required for maternal responses to ultrasonic pup isolation calls,[18] indicating that this brain area might be especially sensitive to oxytocin modulation and important for processing social vocalizations. Previously we generated novel and specific antibodies to the mouse oxytocin receptor[21] and identified an unusual left lateralization of oxytocin receptor expression in female mouse auditory cortex that might promote neural plasticity for recognizing the behavioral meaning of pup calls.[18] However, little is known about the oxytocin receptor expression profile in male cortex, or the relation of oxytocin receptor signaling to male mouse paternal behavior.

We used the most specific antibodies we generated, OXTR-2, to label oxytocin receptors in male mouse left and right auditory cortex (Fig. 1a). We also verified that OXTR-

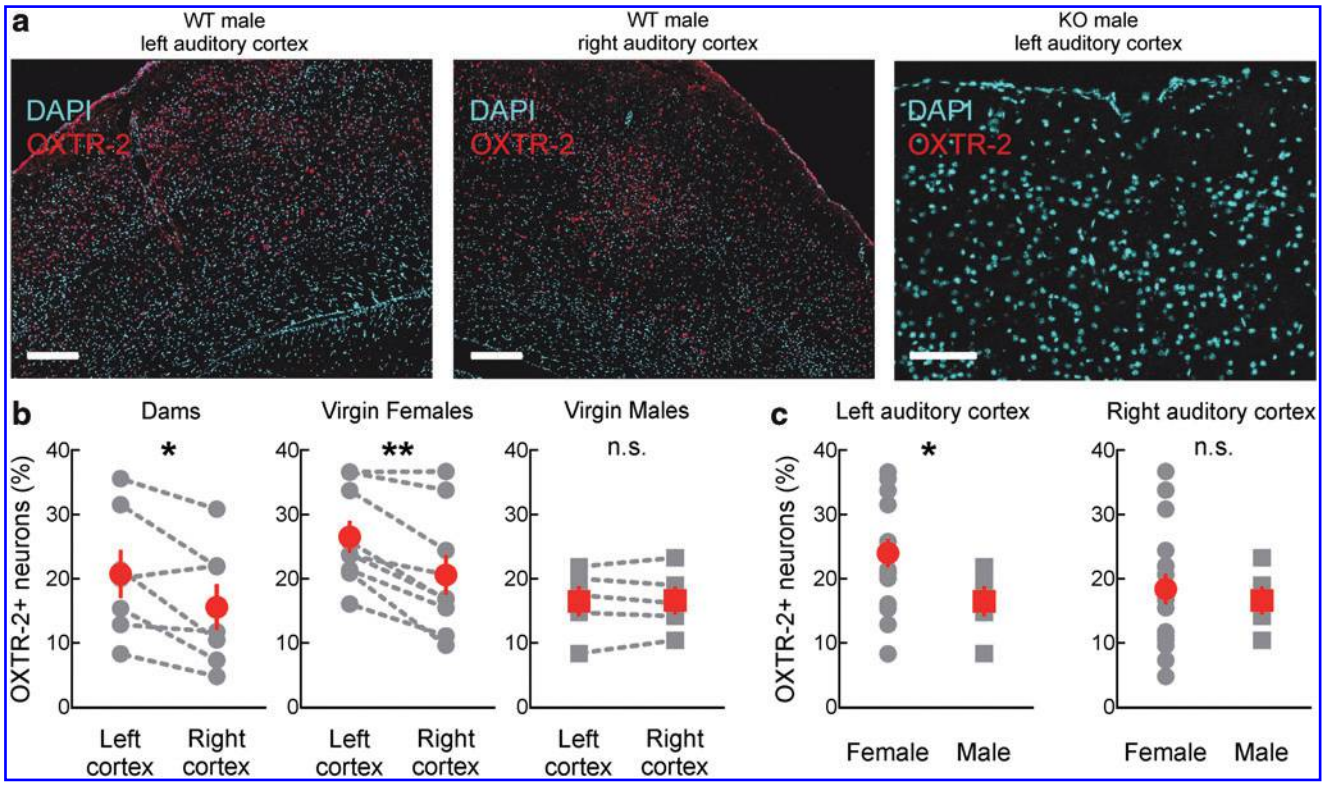

FIG. 1. Oxytocin receptor expression is higher in female mouse left auditory cortex than right or male auditory cortex. **(a)** Immunostained sections of left and right core auditory cortex from same wild-type male (*left* and *middle*, imaged at 10×, scale bars 100 μm), versus oxytocin receptor knockout male (*right*, imaged at 10×, scale bar 100 μm); *red*, OXTR-2; *blue*, DAPI. **(b)** Quantification of oxytocin receptor expressing cells (OXTR-2$^+$) from adult female dams, virgins, and males in left versus right auditory cortex from the same animals. Receptor expression was higher on the left side in dams (left: 20.8% ± 3.7% and right: 15.6% ± 3.6% of DAPI$^+$ cells were OXTR-2$^+$, $N=7$, $p=0.027$ left versus right expression, Student's paired two-tailed *t*-test) and virgins (left: 26.5% ± 2.5% cells and right: 20.6% ± 3.2% cells, $N=9$, $p=0.001$) but not males (left: 16.5% ± 2.4% cells and right: 16.6% ± 2.2% cells, $N=5$, $p=0.866$). *Gray* symbols, individual animals. *Red* symbols, group means. **(c)** Receptor expression was higher in left auditory cortex of females than males (*left*; females: 24.0% ± 2.2% cells, $N=16$, versus males: 16.5% ± 2.4% cells, $N=5$, $p=0.039$, Student's unpaired two-tailed *t*-test), but receptor expression was comparable between males and females in right auditory cortex (*right*, females: 18.4% ± 2.4% cells versus males: 16.6% ± 2.2% cells, $p=0.588$). *$p<0.05$; **$p<0.01$; n.s., not significant. Statistics and error bars are mean ± SEM.

2 was specific for oxytocin receptors in male oxytocin receptor knockout mouse brain (Fig. 1a). OXTR-2 expression was not significantly different across hemispheres in male auditory cortex (Fig. 1b; male left vs. right OXTR-2^+ cells: $p=0.866$), in contrast to the significant left lateralization of OXTR-2 expression in dams and virgin females (Fig. 1b; OXTR-2^+ cells in left vs. right auditory cortex of dams: $p=0.027$ and virgin females: $p=0.001$). Interestingly, this lateralization was due to a higher absolute level of OXTR-2^+ cells in female left auditory cortex than female right auditory cortex or either hemispheres in males (Fig. 1c). In other words, male left and right auditory cortex had a similar (and nonzero) level of oxytocin receptor expression as female right auditory cortex. Consequentially, this suggests that oxytocin might have some function in male auditory cortex and additionally provides an opportunity to probe the functional significance of left-lateralized receptor expression in female auditory cortex.

Cortical oxytocin receptor lateralization in females is developmentally regulated

Next we wondered if the difference in male and female left auditory cortex oxytocin receptor expression was present at birth or emerged over development. Previous studies have shown that oxytocin receptor expression in mouse cortex is highest during the second postnatal week, increasing from birth and then subsequently decreasing to substantially lower levels. In parallel, receptor expression begins highest in superficial and deep cortical layers and then increases in layer 4.[7,21,59] Using OXTR-2 antibodies in tissue sections from animals at the second postnatal week, we found a similar pattern in males. Specifically, the relative fraction of cells expressing oxytocin receptors was much higher in the young brain and comparable between males and females (Fig. 2a).

The laminar organization of receptor expression was also similar in females and males at the second postnatal week, with layer 4 having the fewest number of cells expressing oxytocin receptors (Fig. 2b). This indicates that the lateralization of oxytocin receptor expression evident in the adult female auditory cortex is not apparent at earlier ages when receptor expression levels are highest. Instead, over the first postnatal month, receptor expression drops in male and female left and right auditory cortices, but decreases less in female left auditory cortex compared to greater decreases in female right auditory cortex and male cortex across hemispheres.

We also performed next-generation sequencing to describe the profiles of oxytocin receptor mRNA in male and female auditory cortex (Fig. 2c) and auditory thalamus (Fig. 2d) over postnatal development. When pooled across hemispheres, there was no significant difference between males and females in terms of the developmental trajectories of receptor mRNA levels. In both males and females, relative mRNA levels were lower in the cortex during the first postnatal week, increased during the second postnatal week, and then decreased to adult levels thereafter (Fig. 2c). In contrast, in the thalamic MGB, receptor mRNA levels were initially high in the first postnatal week and then declined (Fig. 2d). These patterns of neurohormone receptor mRNA regulation were specific for oxytocin, as quantification of mRNA for the vasopressin V1a receptor revealed almost zero expression beyond the first postnatal week in cortex (Fig. 2e) and thalamus (Fig. 2f). Therefore, while oxytocin can cross-react and signal through vasopressin receptors in other systems, this is unlikely to occur in the auditory cortex due to lack of vasopressin receptor expression. We also note that while receptor expression depends on mRNA, other cellular factors (e.g., related to mRNA/protein degradation and/or posttranscriptional regulation) are also important for determining how mRNA abundance leads to functional expression of oxytocin receptors.[60,61]

Proteomic effects of oxytocin

Previously we have examined the physiological effects of oxytocin on synaptic transmission in the auditory cortex and other brain areas important for social behavior.[18,21] However, little is known about the signaling systems engaged by G protein-coupled oxytocin receptor activation in the brain. To document the functional consequences of oxytocin receptor signaling, we performed tandem mass tag mass spectrometry and total, as well as phosphoproteomic, analysis.[54–58] This is an unbiased approach that can reveal changes in protein expression levels and phosphorylation events across the proteome. We infused oxytocin directly into the auditory cortex of male and female adult mice *in vivo*, prepared tissue samples with laser microdissection for mass spectrometry, and compared the effects of elevating oxytocin levels in left female versus male auditory cortex.

We first examined changes in total gene expression induced by oxytocin infusion. Out of 3571 proteins, changes in protein levels were reliably quantified for 2696 proteins for which we had multiple samples. While changes in protein level were minimally different in oxytocin-treated male left versus saline-treated right auditory cortex (Fig. 3a), we noticed a strong asymmetry in females, with many more proteins upregulated in left auditory cortex after oxytocin infusion (Fig. 3b; points above the dashed unity line). In total, the expression of 367 proteins was significantly different between female and male left auditory cortex (Fig. 3c and Table 1), including synaptic vesicle proteins such as synaptophysin and VGLUT-2, and components of signal transduction pathways such as PKA.

We then examined phosphorylation events occurring after oxytocin receptor activation. We examined 1325 out of a total of 1794 serine, threonine, and tyrosine phosphosites identified in the combined samples and focused our analysis on 468 phosphosites identified in the complete sample set, because these 468 sites were quantified in all of the replicates. As with total protein expression, phosphorylation occurred symmetrically in male left versus right auditory cortex (Fig. 3d), but was asymmetrical in females such that more phosphorylation occurred in female left than right auditory cortex (Fig. 3e). After Student's *t*-test with Benjamini–Hochberg correction, there were eight sites with statistically-significant differences in phosphorylation ($p<0.05$) between female and male left auditory cortex, including a reduction in phosphorylation of female CaMKIIβ subunits and an increase on clathrin heavy chain 1 (Fig. 3f and Table 2). Thus there are molecular and functional differences between oxytocin receptor activation in left female auditory cortex and other auditory cortical circuits in right female cortex and in males. This lateralized

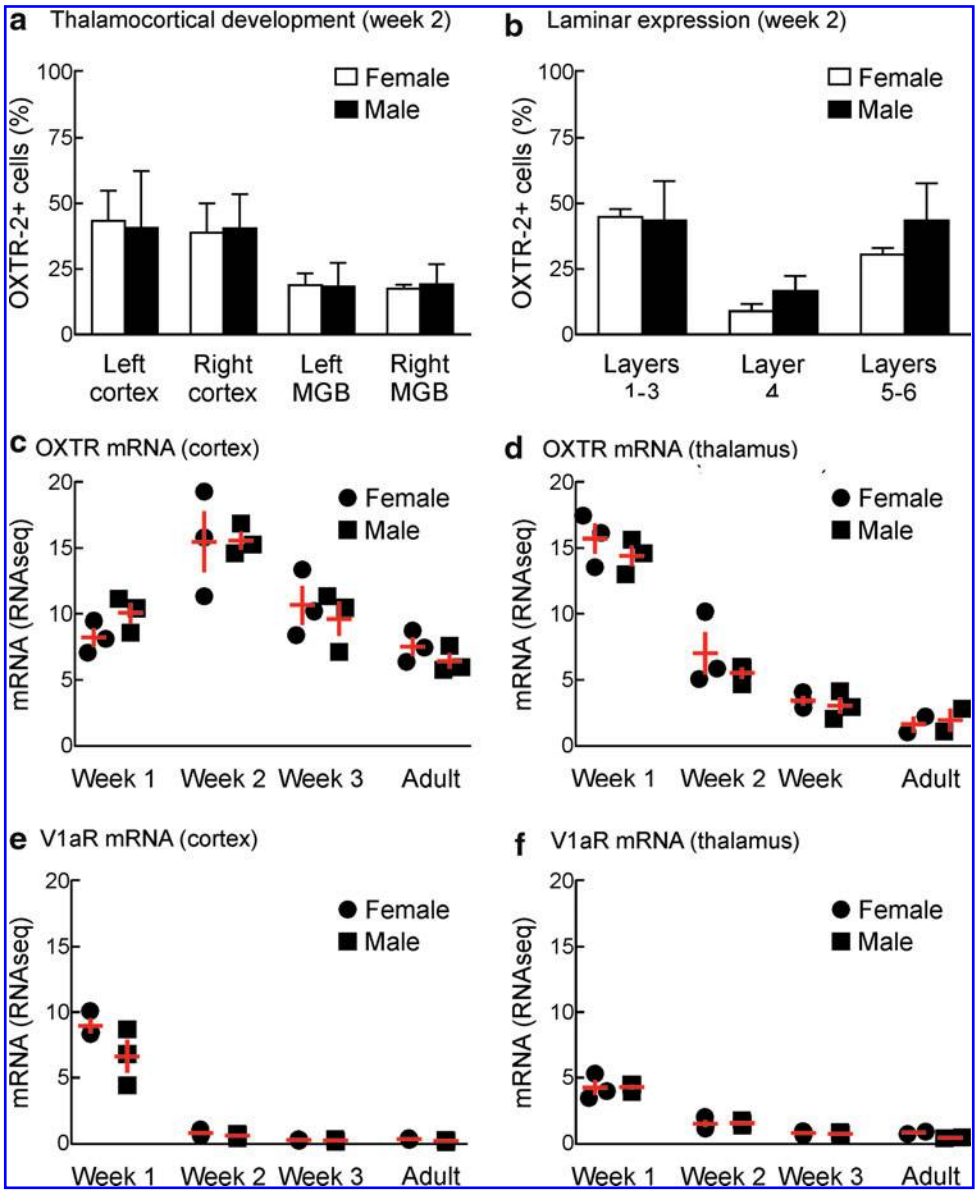

FIG. 2. Asymmetric cortical oxytocin receptor expression in females emerges over postnatal development. **(a)** Oxytocin receptor expression quantified by number of DAPI-stained OXTR-2^+ cells at the second postnatal week of development of mouse auditory cortex and auditory thalamus (MGB). In contrast to receptor expression in adults, oxytocin receptor expression during the second postnatal week is similar in males and females in both cortex (left auditory cortex, females: 43.4% ± 5.7% cells were OXTR-2^+ versus males: 40.7% ± 15.3% cells were OXTR-2^+, $N = 4$ females and $N = 2$ males, $p = 0.900$; right auditory cortex: females: 38.9% ± 5.6% cells versus males: 40.5% ± 9.1% cells, $p = 0.891$) and MGB (left auditory thalamus, females: 18.8% ± 2.3% cells versus males: 18.4% ± 6.3% cells, $N = 4$ females and $N = 2$ males, $p = 0.963$; right auditory thalamus: females: 17.5% ± 0.7% cells versus males: 19.1% ± 5.5% cells, $p = 0.815$). **(b)** During the second postnatal week, oxytocin receptors are expressed in superficial and deeper layers more than in layer 4, in similar levels both in males and females (layers 1–3: females: 38.4% ± 16.8% cells versus males: 43.5% ± 15.0% cells, $N = 4$ females and $N = 4$ males, $p = 0.753$; layer 4: females: 4.9% ± 0.8% cells versus males: 16.7% ± 5.7% cells, $p = 0.127$; layer 5–6: females: 36.4% ± 11.8% cells versus males: 43.4% ± 14.3% cells, $p = 0.600$). **(c)** Normalized mRNA levels for oxytocin receptor in auditory cortex pooled across hemispheres were similar between females (*circles*, $N = 3$ per age group) and males (*squares*, $N = 3$ per age group, $p > 0.9$ compared to age-matched females, ANOVA with Bonferroni correction for multiple comparisons). **(d)** mRNA for oxytocin receptor in MGB was similar between females ($N = 3$ per age group) and males ($N = 2$–3 per age group, $p > 0.9$ compared to age-matched females). **(e)** mRNA for vasopressin V1a receptor in cortex was similar between females and males during the first postnatal week ($N = 3$) and declined to zero later in development and in adults. **(f)** mRNA levels for vasopressin V1a receptor in MGB were also similar between females and males during the first postnatal week ($N = 3$) and declined to zero thereafter. Statistics and error bars are mean ± SEM. MGB, medial geniculate body.

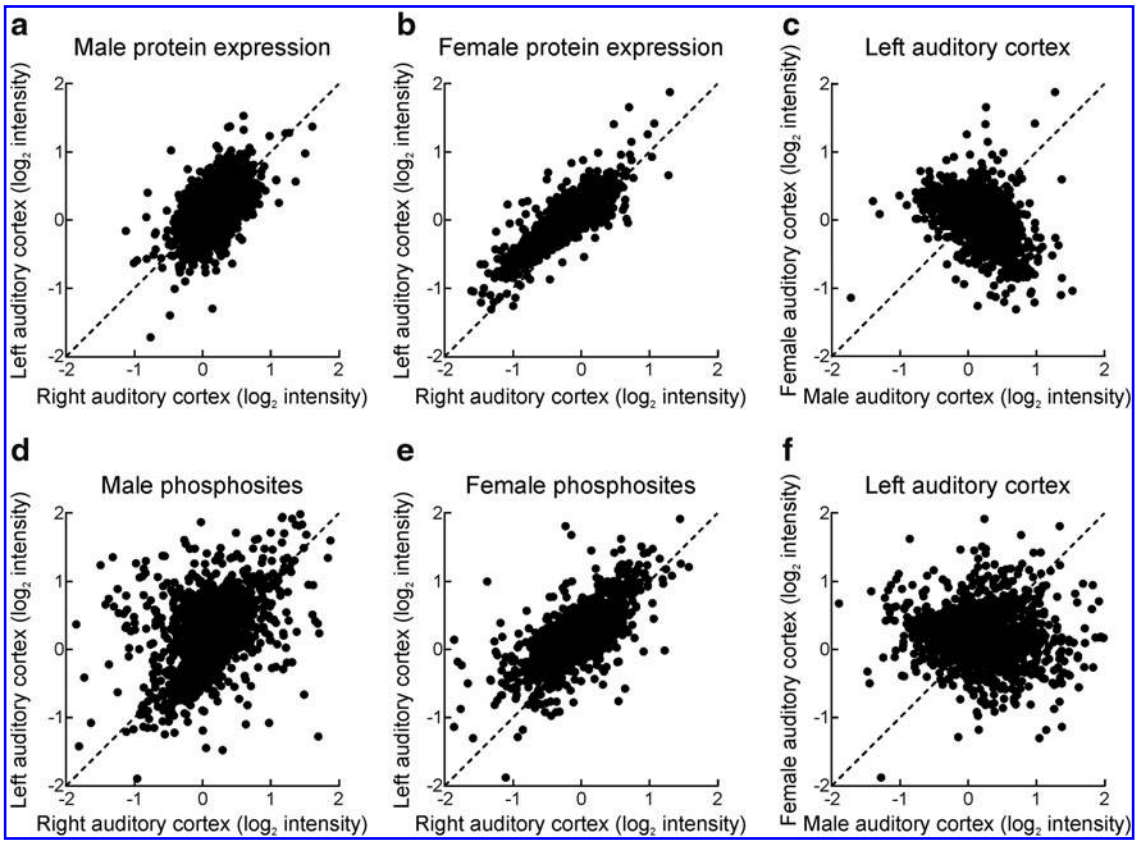

FIG. 3. Proteomic analysis of adult mouse auditory cortex after oxytocin treatment. **(a)** Change in total protein expression for 2,696 out of 3,571 proteins for which multiple peptide counts were detected, in male left versus right auditory cortex after oxytocin infusion (compared to the other hemisphere infused with saline). Protein levels are quantified as $\log_2$ intensity normalized to reference. No significant difference in expression profile was observed in left versus right male auditory cortex. **(b)** Change in protein expression in female left versus right auditory cortex after oxytocin infusion, compared to saline infusion in the other hemisphere. Note more change in expression in left versus right auditory cortex. **(c)** Change in protein expression in the left auditory cortex of females versus males, same data as in **(a, b)** for the left cortex samples. **(d)** Change in serine, threonine, and tyrosine phosphorylation, in male left versus right auditory cortex after oxytocin infusion. Same animals as in **(a)**. No significant difference in phosphorylation was observed in left versus right male auditory cortex. **(e)** Change in phosphorylation levels in female left versus right auditory cortex after oxytocin infusion, compared to saline infusion in the other hemisphere. Note more change in expression in left versus right auditory cortex. Same animals as in **(b)**. **(f)** Change in phosphorylation levels in the left auditory cortex of females versus males, same data as in **(d, e)** for the left cortex samples.

program of phosphorylation and protein expression might relate to the overall higher expression level of oxytocin receptors in female left auditory cortex and also might be related to the heightened plasticity in this brain region for infant vocalizations.[18]

Oxytocin supplements enhance female but not male parental behavior

Given these anatomical and molecular differences, we asked whether oxytocin had similar effects on males and females for enhancing parental behavior. After weaning, mice were isolated from pups and raised to adulthood. Individual adult pup-naive males or females were screened to ensure that they did not initially retrieve pups and then cohoused continuously with litters and dams that were verified to reliably retrieve pups. Retrieval abilities and other types of parental behavior were assessed at regular intervals over a week of cohousing, with some animals receiving systemic oxytocin after each testing session and other animals receiving saline injections.

About half of all male C57BL/6 mice cohoused with experienced dams began retrieving pups after several days (Fig. 4a). Individual male mice began retrieving at various times, with a minority retrieving after <6 h of cohousing ($\sim$15%), and other males requiring more cohousing to begin expressing this behavior. In contrast to the effects of oxytocin treatment on female mice,[18] oxytocin injections did not affect the time course of retrieval. Males receiving oxytocin (Fig. 4a, red) and males receiving saline injections (Fig. 4a, black) began expressing retrieval behavior at approximately the same rates.

In general, male C57BL/6 mice expressed many of the same parenting behaviors as cohoused virgin female mice. We observed that individual cohoused males began crouching and grooming pups around the times that they began reliably retrieving pups during retrieval testing, as with cohoused virgin females. We quantified the rate at which males began collecting bedding and nest building when placed in the retrieval test chamber with pups. Oxytocin-injected and saline-injected males both began nest building at similar rates,

Table 1. List of Proteins Differentially Expressed in Female Versus Male Left Auditory Cortex After Oxytocin Infusion

Gene name	*Protein name*	*Protein Ac#*	*Female/Male*	*Peptides*	*Mol. weight [kDa]*	p-*value*
Acat1	Acetyl-CoA acetyltransferase, mitochondrial	Q8QZT1	0.479701043	18	44.816	0.005555
Actl6b	Actin-like protein 6B	Q99MR0;F8WI57	0.58330749	5	46.891	0.0055632
Actr1a	Alpha-centractin	P61164	0.570887783	8	42.613	0.0277916
Actr1b	Beta-centractin	Q8R5C5	0.599624293	9	42.281	0.0014881
Actr2	Actin-related protein 2	P61161	0.572448861	15	44.76	0.0082061
Actr3	Actin-related protein 3	Q99JY9	0.569281286	18	47.357	0.0052816
Acyp1	Acylphosphatase;Acylphosphatase-1	E9QJT5;P56376;Q8BMV3	0.483779914	2	17.344	0.0182739
Adap1	ArfGAP with dual PH domains 1	E9PY16	0.522056707	6	43.37	0.0012064
Adcy9	Adenylate cyclase type 9	P51830;E9Q706	1.408425958	13	150.95	0.0063146
Add3	Gamma-adducin	Q9QYB5	1.670485472	7	78.776	0.001815
Adk	Adenosine kinase	P55264	0.570092071	8	40.148	0.0001443
Ak1	Adenylate kinase isoenzyme 1	Q9R0Y5	0.471663952	9	21.539	0.0083886
Akap12	A-kinase anchor protein 12	Q9WTQ5	1.708101308	4	180.69	0.0115633
Akr1b1	Aldose reductase	P45376;D3YVJ7	0.563650656	13	35.732	0.0055564
Aldh2	Aldehyde dehydrogenase, mitochondrial	P47738	0.608954098	15	56.537	0.0228039
Aldh7a1	Alpha-aminoadipic semialdehyde dehydrogenase	Q9DBF1;G3UYR8	0.592718317	18	58.861	0.0065916
Aldoc	Fructose-bisphosphate aldolase C	P05063	0.601927407	25	39.394	0.0208794
Ank1	Ankyrin-1	G5E8J2;B7ZW98;E9QNT8;D3YTV8; Q0VGY9;Q02357;G8JL84;D3Z5 M4;G3UY11	1.58202815	17	202.52	0.0001047
Ankmy2	Ankyrin repeat and MYND domain-containing protein 2	Q3TPE9	0.697983458	3	48.774	0.0050031
Anp32a	Acidic leucine-rich nuclear phosphoprotein 32 family member A	O35381;D3Z7 M9;F6UFG6;D3YYE1	0.476439183	9	28.537	0.0092146
Aplp2	Amyloid-like protein 2	Q60709;Q06335	0.436695118	7	85.247	0.0118786
Apoo	Apolipoprotein O	Q9D186;B1ASQ2;Q9DCZ4	0.461733958	4	18.798	0.0145509
Aqp4	Aquaporin-4	P55088	1.942386674	2	34.436	0.0081357
Arf1	ADP-ribosylation factor 1;ADP-ribosylation factor 3;ADP-ribosylation factor 2	P84078;P61205;Q8BSL7	0.584878944	8	20.697	0.0093598
Arf5	ADP-ribosylation factor 5	P84084	0.619919866	7	20.529	0.0136205
Arfgap1	ADP-ribosylation factor GTPase-activating protein 1	Q3TGS9;V9GWV1;V9GXM1;Q9EPJ9	0.664716223	10	43.183	0.0104055
Arhgdia	Rho GDP-dissociation inhibitor 1	Q99PT1	0.56259373	8	23.407	0.0082236
Arl6ip1	ADP-ribosylation factor-like protein 6-interacting protein 1	Q9JKW0	0.666926566	2	23.437	0.0003182
Arl8a	ADP-ribosylation factor-like protein 8A; ADP-ribosylation factor-like protein 8B	F6QKK2;Q8VEH3;Q9CQW2	0.675885464	3	18.756	0.0022909
Armc1	Armadillo repeat-containing protein 1	Q9D7A8	0.613337503	4	31.246	0.018742
Arpc3	Actin-related protein 2/3 complex subunit 3	D3Z2F7;D3Z2F8;H7BWZ3;Q9JM76	0.45582181	5	18.682	0.0226217
Arpc4	Actin-related protein 2/3 complex subunit 4	P59999	0.493412807	7	19.667	0.0017905
Asrgl1	Isoaspartyl peptidase/L-asparaginase;Isoaspartyl peptidase/L-asparaginase alpha chain;Isoaspartyl peptidase/L-asparaginase beta chain	Q8C0 M9	0.582788463	13	33.95	0.0150316
Atg3	Ubiquitin-like-conjugating enzyme ATG3	Q9CPX6	0.600348905	3	35.796	0.0129143

(*continued*)

Table 1. (Continued)

Gene name	*Protein name*	*Protein Ac#*	*Female/Male*	*Peptides*	*Mol. weight [kDa]*	p-*value*
Atp12a	Potassium-transporting ATPase alpha chain 2	Q9Z1 W8	2.059596745	7	114.73	0.0003209
Atp5d	ATP synthase subunit delta, mitochondrial	Q9D3D9	0.473100043	2	17.6	0.0117837
Atp5e	ATP synthase subunit epsilon, mitochondrial	P56382	0.358646548	4	5.8378	0.0006655
Atp5i	ATP synthase subunit e, mitochondrial	Q06185;Q8BTB6	0.375944908	4	8.2355	0.0100067
Atp6v1c1	V-type proton ATPase subunit C 1	Q9Z1G3	0.572822473	22	43.887	0.0090397
Atp6v1f	V-type proton ATPase subunit F	Q9D1K2;F7B2B4	0.396285077	4	13.37	0.0050039
Atpif1	ATPase inhibitor, mitochondrial	E9PV44;O35143	0.251149921	3	8.7887	0.004043
Atrx	Transcriptional regulator ATRX	Q61687;F6RDB7	1.888116367	2	278.58	0.0313263
Basp1	Brain acid soluble protein 1	Q91XV3	0.213354693	21	22.086	0.0007824
Baz1b	Tyrosine-protein kinase BAZ1B	Q9Z277	0.600555436	2	170.65	0.0088674
Bcam	Basal cell adhesion molecule	Q9R069	1.587341241	4	67.669	0.016151
Bdh1	D-beta-hydroxybutyrate dehydrogenase, mitochondrial	Q80XN0;D3Z2Y8	0.530761235	10	38.299	0.0193542
Bpnt1	3(2),5-bisphosphate nucleotidase 1	Q9Z0S1;D3Z0E6	0.494105957	11	33.196	0.0063535
Bsg	Basigin	K3 W4Q8;P18572;J3QP71	0.636091937	7	24.116	0.0114208
Cab39	Calcium-binding protein 39	Q06138;D3YV52	0.543161135	6	39.842	0.013336
Calb1	Calbindin	P12658	0.452497831	7	29.994	0.0019002
Calb2	Calretinin	Q08331	0.323074798	10	31.372	0.0314436
Calr	Calreticulin	P14211	0.542040144	13	47.994	0.0008495
Caprin1	Caprin-1	Q60865	0.675781818	7	78.168	0.008968
Capzb		A2AMW0;F7CAZ6	0.505602037	14	29.295	0.0279998
Ccdc93	Coiled-coil domain-containing protein 93	E9QAD4;Q7TQK5	1.87606658	3	72.474	0.0039933
Cd47	Leukocyte surface antigen CD47	Q61735;D3Z187	0.67246774	4	33.097	0.0120762
Cdc37	Hsp90 co-chaperone Cdc37;Hsp90 co-chaperone Cdc37, N-terminally processed	Q61081	0.563169098	10	44.593	0.0069542
Cdc42	Cell division control protein 42 homolog	P60766	0.453927074	6	21.258	0.0046324
Cdv3	Protein CDV3	A0A087WNP6;Q4VAA2;A0A087WRM0	0.37181297	4	24.196	0.003128
Celf1	CUGBP Elav-like family member 1	P28659	0.632006275	7	52.107	0.0130236
Cfl1	Cofilin-1	P18760;F8WGL3	0.321583089	13	18.559	0.0018601
Cfl2	Cofilin-2	P45591	0.494212012	8	18.709	0.005649
Chmp4b	Charged multivesicular body protein 4b	Q9D8B3	0.481898809	4	24.936	0.0016647
Chmp6	Charged multivesicular body protein 6	P0C0A3;B1AZ42	0.603162814	4	23.415	0.0194772
Cirbp	Cold-inducible RNA-binding protein	P60824;K4DI65	0.343375128	2	18.607	0.0436636
Cldn11	Claudin-11	Q60771	2.305076439	4	22.114	0.0246023
Clta	Clathrin light chain A	B1AWD8;B1AWD9;O08585;B1AWE0; Q6PFA2;B1AWE1	0.317105696	10	25.661	0.0010564
Cltb	Clathrin light chain B	Q6IRU5;F7BHJ0	0.353466383	8	25.171	0.0105426
Cmpk1	UMP-CMP kinase	Q9DBP5	0.491562261	7	22.165	0.0075233
Cmtr1	Cap-specific mRNA (nucleoside-2-O-)-methyltransferase 1	Q9DBC3	1.559490556	4	95.675	0.0130812
Cndp2	Cytosolic nonspecific dipeptidase	Q9D1A2	0.748651061	7	52.767	0.001565
Cnrip1	CB1 cannabinoid receptor-interacting protein 1	Q5 M8 N0;F7C0H6	0.489892742	5	18.612	0.0038416
Cntn2	Contactin-2	Q61330;A0A087WQQ9	1.650088858	7	113.22	0.0229728
Cntnap2	Contactin-associated protein-like 2	E9QNF7;Q9CPW0	1.498907732	11	148.25	0.0125282

(*continued*)

Table 1. (Continued)

Gene name	*Protein name*	*Protein Ac#*	*Female/Male*	*Peptides*	*Mol. weight [kDa]*	p-*value*
Copz1	Coatomer subunit zeta-1	P61924	0.448284654	2	20.198	0.0091487
Coro1a	Coronin-1A;Coronin	O89053;G3UYK8	0.67268752	23	50.989	0.005239
Cotl1	Coactosin-like protein	Q9CQI6	0.537680319	9	15.944	0.021899
Cox6a1	Cytochrome c oxidase subunit 6A, mitochondrial;Cytochrome c oxidase subunit 6A1, mitochondrial	Q9DCW5;P43024	0.545169892	2	12.483	0.0001726
Cox6b1	Cytochrome c oxidase subunit 6B1	P56391	0.670085016	6	10.071	0.0019601
Cox7c	Cytochrome c oxidase subunit 7C, mitochondrial	P17665	0.47392973	2	7.3325	0.0024505
Cplx2	Complexin-2	P84086	0.351799619	3	15.394	0.0099193
Cpt2	Carnitine O-palmitoyltransferase 2, mitochondrial	P52825	1.459716289	4	73.98	0.0145956
Ctsd	Cathepsin D	P18242;F8WIR1;F6Y6 L6	0.606544571	6	44.953	0.0024779
D10Jhu81e	ES1 protein homolog, mitochondrial	Q9D172	0.591821755	8	28.09	0.0107644
Dazap1	DAZ-associated protein 1	Q3UGB5;Q9JII5;D3Z4J1	0.552647241	4	43.157	0.0009669
Dctn3	Dynactin subunit 3	Q9Z0Y1;E9Q919	0.57366434	7	20.978	0.0125385
Dcun1d2	DCN1-like protein;DCN1-like protein 2	G5E8Q5;G5E8Q6;Q8BZJ7	0.308324897	3	22.769	0.0065595
Ddt	D-dopachrome decarboxylase	O35215;G3UZN1;G3UYJ7	0.359536775	4	13.077	9.215E-05
Dgkb	Diacylglycerol kinase beta	Q6NS52	1.514639258	6	90.271	0.00125
Diap2	Protein diaphanous homolog 2	Q6 W4 W7;E9Q4 U7;O70566	1.407022368	3	125.38	0.006141
Dip2a	Disco-interacting protein 2 homolog A	F8WI56;D3Z7D3;Q8BWT5	1.700708085	10	169.52	0.0096114
Dmtn	Dematin	Q9WV69	0.631388403	7	45.468	0.0064477
Dnajc8	DnaJ homolog subfamily C member 8	A2ALF0;A2ALF3;F6TQL3;Q6NZB0	0.570565593	2	25.835	0.0258117
Dpp8	Dipeptidyl peptidase 8	Q80YA7	1.593485858	3	102.18	0.0018497
Drg1	Developmentally-regulated GTP-binding protein 1	P32233	0.628594185	5	40.512	0.0038075
Dstn	Destrin	Q9R0P5	0.400117437	7	18.521	0.0022254
Dynll1	Dynein light chain 1, cytoplasmic	P63168;Q80ZS7	0.380219517	7	10.366	0.0074183
Eef1b	Elongation factor 1-beta	O70251;A0A087WS46	0.33195184	3	24.693	0.0003744
Eef1g	Elongation factor 1-gamma	Q9D8 N0	0.581289097	17	50.06	0.0118851
Efhd2	EF-hand domain-containing protein D2	Q8C845;Q9D8Y0	0.543069705	14	26.8	0.023187
Eif3k	Eukaryotic translation initiation factor 3 subunit K	Q9DBZ5	0.446971063	3	25.086	0.0021625
Eif5a	Eukaryotic translation initiation factor 5A; Eukaryotic translation initiation factor 5A-1;Eukaryotic translation initiation factor 5A-2	A0A0A0MQM0;P63242;J3QPS8;Q8BGY2	0.31425582	4	16.302	0.0008346
Elavl1	ELAV-like protein 1	P70372	0.658924218	9	36.169	0.0103226
Elavl4	ELAV-like protein;ELAV-like protein 4	A2A9S3;A2A9S2;A2A9R8;A2A9R6; Q8BVA9;A2A9S0;Q61701	0.544051229	11	39.269	0.0220808
Eno1	Alpha-enolase	P17182;Q6PHC1	0.525727019	24	47.14	0.0063183
Eno2	Gamma-enolase;Enolase	P17183;D3Z6E4	0.550088029	15	47.296	0.0173807
Eri3	ERI1 exoribonuclease 3	Q8C460	0.526605716	3	37.189	0.0044623
Fabp3	Fatty acid-binding protein, heart	P11404	0.534760745	5	14.819	0.0277557
Fabp5	Fatty acid-binding protein, epidermal	Q05816	0.447569582	8	15.137	0.0011793
Fabp7	Fatty acid-binding protein, brain	E9Q0H6;P51880	0.345431528	3	20.615	0.046509
Fech	Ferrochelatase;Ferrochelatase, mitochondrial	Q544X6;P22315	0.645394448	9	47.421	0.0117111
Fh	Fumarate hydratase, mitochondrial	P97807	0.596275469	15	54.356	0.0228899

(*continued*)

Table 1. (Continued)

Gene name	*Protein name*	*Protein Ac#*	*Female/Male*	*Peptides*	*Mol. weight [kDa]*	p-*value*
Fkbp2	Peptidyl-prolyl cis-trans isomerase FKBP2	P45878	0.658754077	2	15.344	0.003848
Fth1	Ferritin heavy chain;Ferritin heavy chain, N-terminally processed	P09528	0.679483286	5	21.066	0.014879
Fxyd7	FXYD domain-containing ion transport regulator 7	P59648	2.012158901	2	8.4867	0.0005354
Gad1	Glutamate decarboxylase 1	P48318	1.404856918	9	66.648	0.005579
Gap43	Neuromodulin	P06837	0.423253611	15	23.632	0.026542
Gapdh	Glyceraldehyde-3-phosphate dehydrogenase	P16858;A0A0A0MQF6;S4R257;D3YYI5	0.637461371	17	35.81	0.0140183
Gas7	Growth arrest-specific protein 7	B1ATI9;Q3 U432;Q60780	0.511928216	9	47.261	0.0126359
Gdi2	Rab GDP dissociation inhibitor beta	Q61598	0.581895893	21	50.537	0.0019597
Gfm1	Elongation factor G, mitochondrial	Q8K0D5	1.566927134	3	83.549	0.0143084
Gga3	ADP-ribosylation factor-binding protein GGA3	S4R2D2;A2A9 W7;Q8BMI3;A2A9 W5	1.82930255	4	64.524	0.0080134
Glo1	Lactoylglutathione lyase	Q9CPU0	0.517703137	6	20.809	0.0005683
Glul	Glutamine synthetase	P15105	0.641076535	21	42.119	0.0121426
Gm9755;Tufm	Elongation factor Tu;Elongation factor Tu, mitochondrial	D3YVN7;Q8BFR5	0.596200452	18	49.538	0.009272
Gmfb	Glia maturation factor beta	Q9CQI3	0.372010713	4	16.723	0.0072571
Gmpr2	GMP reductase 2	Q99 L27	0.561386863	3	38.018	0.0041546
Gna11	Guanine nucleotide-binding protein subunit alpha-11	P21278	0.620880748	10	42.024	0.022949
Gnb2	Guanine nucleotide-binding protein G(I)/G(S)/G(T) subunit beta-2	P62880;D3Z1 M1;E9QKR0;D3Z1T4;D3YZX3	0.467799368	12	37.331	0.0060141
Gnb4	Guanine nucleotide-binding protein subunit beta-4	P29387	0.432955891	11	37.379	0.0209385
Got1	Aspartate aminotransferase, cytoplasmic	P05201	0.630048536	22	46.247	0.0085664
Gpi	Glucose-6-phosphate isomerase	P06745;F6SAC3	0.622915679	25	62.766	0.0077953
Grb2	Growth factor receptor-bound protein 2	B1AT92;Q60631	0.596188366	12	23.587	0.0202182
Gsg1l	Germ cell-specific gene 1-like protein	D3Z7H4	1.989599065	2	35.889	0.0132011
Gsk3b	Glycogen synthase kinase-3 beta	E9QAQ5;Q9WV60	0.666702205	13	47.989	0.0166468
Gsta4	Glutathione S-transferase A4	P24472	0.554654659	7	25.564	0.0292558
Gstp1	Glutathione S-transferase P 1	P19157	0.605443099	5	23.609	0.0057487
Hacd2	Very-long-chain (3R)-3-hydroxyacyl-CoA dehydratase 2	Q9D3B1	1.79382861	2	28.402	0.0222001
Hdgfrp3	Hepatoma-derived growth factor-related protein 3	Q9JMG7	0.333211572	4	22.43	0.0054704
Hdhd2	Haloacid dehalogenase-like hydrolase domain-containing protein 2	Q3UGR5	0.47114615	3	28.73	0.0031718
Hebp1	Heme-binding protein 1	Q9R257	0.548684762	6	21.067	0.0304064
Hepacam	Hepatocyte cell adhesion molecule	Q640R3	1.664958651	5	46.366	0.0042403
Hint1	Histidine triad nucleotide-binding protein 1	P70349;B0R1E3	0.417765866	5	13.777	0.0092147
Hint2	Histidine triad nucleotide-binding protein 2, mitochondrial	Q9D0S9	0.504710119	5	17.32	0.0062089
Hint3	Histidine triad nucleotide-binding protein 3	F8WH96;Q9CPS6	0.536154155	2	18.518	0.0055668
Hist1 h1d	Histone H1.3	P43277	0.562576127	14	22.099	0.0257562
Hist1 h3b	Histone H3.2;Histone H3.1;Histone H3;Histone H3.3;Histone H3.3C	P84228;P68433;F8WI35;P84244;P02301;E0CZ27	0.496672556	6	15.388	0.00344
Hist1 h4a	Histone H4	P62806	0.494440749	10	11.367	0.0103604

(*continued*)

Table 1. (Continued)

Gene name	*Protein name*	*Protein Ac#*	*Female/Male*	*Peptides*	*Mol. weight [kDa]*	p-*value*
Hmgb1	High mobility group protein B1	P63158;D3YZ18;D3YVC6	0.419206763	7	24.893	0.0176376
Hmgcl	Hydroxymethylglutaryl-CoA lyase, mitochondrial	P38060	0.546428459	6	34.238	0.029799
Hnrnpa1	Heterogeneous nuclear ribonucleoprotein A1;Heterogeneous nuclear ribonucleoprotein A1, N-terminally processed	Q5EBP8;P49312	0.62884729	11	38.833	0.0118271
Hnrnpa2b1	Heterogeneous nuclear ribonucleoproteins A2/B1	O88569	0.610989923	22	37.402	0.0050472
Hnrnpab	Heterogeneous nuclear ribonucleoprotein A/B	Q99020;Q80XR6;Q20BD0	0.384624081	6	30.831	0.0049469
Hnrnpd	Heterogeneous nuclear ribonucleoprotein D0	Q60668;F6ZV59;G5E8G0;G3X9 W0;E9Q5B6	0.534864094	6	38.354	0.0050086
Hnrnpdl	Heterogeneous nuclear ribonucleoprotein D-like	D3YTQ3;F6VQH5;Q9Z130	0.474595509	6	46.27	0.0053067
Hnrnph3	Heterogeneous nuclear ribonucleoprotein H3	D3YWT1;D3Z3 N4	0.665078389	6	35.181	0.0136856
Hpca	Neuron-specific calcium-binding protein hippocalcin	E9PV73;P84075;A2A7R5	0.396686951	10	21.82	0.0001097
Hspe1	10 kDa heat shock protein, mitochondrial	Q64433	0.254110536	10	10.963	0.0015615
Idh1	Isocitrate dehydrogenase [NADP] cytoplasmic	O88844;A0A087WPT4;A0A087WRS9	0.508003645	14	46.674	0.0076134
Idh3a	Isocitrate dehydrogenase [NAD] subunit alpha, mitochondrial	Q9D6R2	0.529882493	18	39.638	0.0119499
Idi1	Isopentenyl-diphosphate Delta-isomerase 1	G3XA48;P58044	0.621835582	2	32.477	0.0100043
Impact	Protein IMPACT	O55091	0.523243698	10	36.276	0.019615
Inf2	Inverted formin-2	E9QLA5;Q0GNC1	2.451039562	3	138.36	0.0008257
Inpp1	Inositol polyphosphate 1-phosphatase	P49442	0.656812901	5	43.346	0.0110766
Iqgap2	Ras GTPase-activating-like protein IQGAP2	Q3UQ44	1.520434099	4	180.53	0.0165929
Kbtbd11	Kelch repeat and BTB domain-containing protein 11	Q8BNW9	1.448813981	12	67.945	0.0108523
Kcnj10	ATP-sensitive inward rectifier potassium channel 10	Q9JM63	1.698336116	2	42.432	0.004827
Khdrbs3	KH domain-containing, RNA-binding, signal transduction-associated protein 3	Q9R226	0.42366687	3	38.807	0.0064267
Kiaa0513	Uncharacterized protein KIAA0513	Q8R0A7;Q3TA40;Q8BQB5	0.580510097	16	46.318	0.0237823
Lasp1	LIM and SH3 domain protein 1	Q61792;A2A6H0;A2A6G9	0.433555704	15	29.994	0.0031263
Ldha	L-lactate dehydrogenase;L-lactate dehydrogenase A chain	G5E8 N5;P06151;D3Z736;D3YZQ9	0.527165303	14	39.758	0.0018064
Lypla1	Acyl-protein thioesterase 1	D3Z269;D3YUG4;D3Z111;J3QP56;P97823	0.52156161	2	14.801	0.0277142
Mag	Myelin-associated glycoprotein	Q3ZB60;A0A087WPR1;P20917	1.93256681	8	62.587	0.0297666
Map1lc3a	Microtubule-associated proteins 1A/1B light chain 3A	Q91VR7;J3QN16	0.546066165	3	14.272	0.0193955
Map2k1	Dual specificity mitogen-activated protein kinase kinase 1	P31938	0.529405521	13	43.474	0.0143403
Mapk10	Mitogen-activated protein kinase;Mitogen-activated protein kinase 10	Q3TQZ7;Q80 W82;Q78GB8;Q8C9D4;Q80 W80;E9QN59;Q61831	0.563237973	5	48.003	0.0180387
Mapk8ip3	C-Jun-amino-terminal kinase-interacting protein 3	E9Q6B6;E9Q6E0;J3QNR6;K3 W4S4;Q9ESN9	2.037333581	8	143.44	0.0372656
Mapre1	Microtubule-associated protein RP/EB family member 1	Q61166	0.585492714	8	30.016	0.0263541

(*continued*)

Table 1. (Continued)

Gene name	*Protein name*	*Protein Ac#*	*Female/Male*	*Peptides*	*Mol. weight [kDa]*	p-*value*
Mapre2	Microtubule-associated protein RP/EB family member 2	D3YYK8;E9Q6X0;Q8R001;Q3TG90	0.641489143	11	29.425	0.0150517
Mapre3	Microtubule-associated protein RP/EB family member 3	Q6PER3	0.595137566	13	31.966	0.0066188
Mapt	Microtubule-associated protein;Microtubule-associated protein tau	A0A0A0MQC7;A2A5Y6;P10637	0.633944115	22	76.259	0.0138399
Mat2a	S-adenosylmethionine synthase isoform type-2	Q3THS6	0.693098184	7	43.688	0.0023354
Mdh1	Malate dehydrogenase, cytoplasmic	P14152	0.497462023	16	36.511	0.0051267
Mdh2	Malate dehydrogenase, mitochondrial	P08249	0.553466164	18	35.611	0.0196021
Mical3	Protein-methionine sulfoxide oxidase MICAL3	Q8CJ19	1.332565553	10	223.72	0.0036979
Mpp1	55 kDa erythrocyte membrane protein	B7ZCL8;A2AN84;P70290;B7ZCM0	1.649672055	4	49.784	0.0203162
Mtmr2	Myotubularin-related protein 2	Q9Z2D1;Q6P572	1.770274813	3	73.231	0.0026572
Mtpn	Myotrophin	P62774	0.383681798	2	12.861	0.0379083
Myh14	Myosin-14	K3 W4R2;Q6URW6	1.609558373	11	228.56	0.0220292
Myl6	Myosin light polypeptide 6	Q60605	0.471166602	5	16.93	0.0123121
Naca	Nascent polypeptide-associated complex subunit alpha;Nascent polypeptide-associated complex subunit alpha, muscle-specific form	Q60817;P70670	0.392709499	4	23.384	0.0065647
Nap1l4	Nucleosome assembly protein 1-like 4	Q78ZA7	0.595194612	6	42.679	0.0202094
Napg	Gamma-soluble NSF attachment protein	Q9CWZ7;D3Z4B2	0.518445261	17	34.732	0.0034402
Ncan	Neurocan core protein	P55066	1.529379236	29	137.2	0.0028904
Nceh1	Neutral cholesterol ester hydrolase 1	Q8BLF1;Q8BYQ0	0.63374244	6	45.739	0.0038475
Ndrg2	Protein NDRG2	Q9QYG0	0.677940368	8	40.789	0.0030703
Ndrg4	Protein NDRG4	Q8BTG7	0.539745154	4	38.508	0.0302889
Ndufa4	Cytochrome c oxidase subunit NDUFA4	Q62425	0.449644904	5	9.3267	0.0041103
Ndufb3	NADH dehydrogenase [ubiquinone] 1 beta subcomplex subunit 3	Q9CQZ6	0.65383989	3	11.692	0.001298
Ndufb4	NADH dehydrogenase [ubiquinone] 1 beta subcomplex subunit 4	Q9CQC7	0.503603898	4	15.081	0.0142853
Ndufb5	NADH dehydrogenase [ubiquinone] 1 beta subcomplex subunit 5, mitochondrial	D3Z568;Q9CQH3;F6Y6 V5;D3YX99; D3Z6 W9	0.491555979	4	14.038	0.0127734
Ndufb6	NADH dehydrogenase [ubiquinone] 1 beta subcomplex subunit 6	A2AP32;Q3UIU2	0.580527238	3	11.741	0.0126429
Ndufs4	NADH dehydrogenase [ubiquinone] iron-sulfur protein 4, mitochondrial	E9QPX3;Q9CXZ1	0.527858761	3	19.803	0.0159454
Ndufs8	NADH dehydrogenase [ubiquinone] iron-sulfur protein 8, mitochondrial	Q8K3J1	0.50460726	7	24.038	0.0230526
Ndufv2	NADH dehydrogenase [ubiquinone] flavoprotein 2, mitochondrial	Q9D6J6;M0QWP9	0.514615171	6	27.285	0.0040931
Necap1	Adaptin ear-binding coat-associated protein 1	Q9CR95	0.561948243	5	29.639	0.0092684
Nfu1	NFU1 iron-sulfur cluster scaffold homolog, mitochondrial	Q9QZ23	0.635050421	3	28.567	0.0035665
Nme2	Nucleoside diphosphate kinase;Nucleoside diphosphate kinase B	E9PZF0;Q01768;Q5NC80;Q5NC79	0.496704622	10	30.2	0.0007879

(*continued*)

Table 1. (Continued)

Gene name	*Protein name*	*Protein Ac#*	*Female/Male*	*Peptides*	*Mol. weight [kDa]*	p-*value*
Npm1	Nucleophosmin	Q9DAY9;E9Q5T3;Q5SQB5;Q61937; Q5SQB0	0.376271845	7	28.385	0.0009471
Nrgn	Neurogranin;NEUG(55-78)	P60761	1.621624186	3	7.4963	0.005263
Nt5c	5(3)-deoxyribonucleotidase, cytosolic type	A2A9X5;Q9JM14	0.532297499	4	21.939	0.0015657
Nucb1	Nucleobindin-1	Q02819;D3Z1 N1;D3Z7D7;H3BK79	0.684738051	2	53.408	0.0076616
Nucks1	Nuclear ubiquitous casein and cyclin-dependent kinase substrate 1	A0A087WRY3;Q80XU3	0.219915355	3	26.184	0.0131669
Nudc	Nuclear migration protein nudC	O35685	0.594521153	11	38.358	0.0192757
Ola1	Obg-like ATPase 1	Q9CZ30;B1AYJ9	0.471903361	9	44.729	0.0015268
Osbpl1a	Oxysterol-binding protein;Oxysterol-binding protein-related protein 1	Q3 V156;Q91XL9;D3Z7I9	0.579958799	5	63.433	0.0002422
Oxct1	Succinyl-CoA:3-ketoacid coenzyme A transferase 1, mitochondrial;Succinyl-CoA:3-ketoacid-coenzyme A transferase	Q9D0K2;Q3UJQ9	0.668894832	13	55.988	0.0064
Pa2 g4	Proliferation-associated protein 2G4	P50580;D3YVH7	0.627787894	12	43.698	0.0207447
Palm	Paralemmin-1	Q9Z0P4	0.613408189	16	41.614	0.0105979
Park7	Protein deglycase DJ-1	Q99LX0;A2A813;A2A815;A2A817; A2A816	0.638851349	10	20.021	0.0138328
Pcbp1	Poly(rC)-binding protein 1	P60335	0.663293939	12	37.497	0.0126623
Pdia6	Protein disulfide-isomerase A6	Q3TML0;Q922R8	0.53158228	10	48.689	0.019028
Pdk3	[Pyruvate dehydrogenase (acetyl-transferring)] kinase isozyme 3, mitochondrial	Q922H2	0.693590579	6	47.922	0.0100667
Pea15	Astrocytic phosphoprotein PEA-15	Q62048;D3Z375	0.180586829	4	15.054	0.0073265
Pebp1	Phosphatidylethanolamine-binding protein 1;Hippocampal cholinergic neurostimulating peptide	P70296;D3Z1 V4;D6RHS6	0.341253136	6	20.83	0.0084573
Pfdn1	Prefoldin subunit 1	Q9CQF7;Q9CWM4	0.417998272	4	14.255	0.0029117
Pfn2	Profilin-2;Profilin	Q9JJV2;D3YWS3	0.414300628	7	15.032	0.0104867
Pgd	6-phosphogluconate dehydrogenase, decarboxylating	Q9DCD0	0.580946316	13	53.247	0.0167994
Pgk1	Phosphoglycerate kinase 1;Phosphoglycerate kinase	P09411;S4R2 M7	0.592478579	25	44.55	0.0224106
Phyhip	Phytanoyl-CoA hydroxylase-interacting protein	Q8K0S0	0.61162732	15	37.554	0.0189116
Pitpna	Phosphatidylinositol transfer protein alpha isoform	P53810;J3QQ30;J3QPW1	0.48562695	16	31.893	0.0033956
Pitpnc1	Cytoplasmic phosphatidylinositol transfer protein 1	A0A0A0MQ88;Q8K4R4;X1WI19	0.571483721	4	35.581	0.0252168
Pnpo	Pyridoxine-5-phosphate oxidase	Q91XF0	0.626454563	2	30.114	0.0107066
Ppa1	Inorganic pyrophosphatase	Q9D819	0.493828406	5	32.667	0.0233225
Ppa2	Inorganic pyrophosphatase 2, mitochondrial	D3Z636;Q91VM9	0.626398799	6	37.985	0.0076608
Ppia	Peptidyl-prolyl cis-trans isomerase A;Peptidyl-prolyl cis-trans isomerase A, N-terminally processed;Peptidyl-prolyl cis-trans isomerase	P17742;F8VPN3	0.470696638	11	17.971	0.0027384
Ppid	Peptidyl-prolyl cis-trans isomerase D	Q9CR16	0.526138302	10	40.742	0.0199667
Ppm1a	Protein phosphatase 1A	P49443	0.587396905	11	42.432	0.0176646
Ppm1g	Protein phosphatase 1G	Q61074	0.72847848	6	58.727	0.005522

(*continued*)

Table 1. (Continued)

Gene name	*Protein name*	*Protein Ac#*	*Female/Male*	*Peptides*	*Mol. weight [kDa]*	p-*value*
Ppme1	Protein phosphatase methylesterase 1	Q8BVQ5	0.576735817	9	42.256	0.0128169
Ppp1ca	Serine/threonine-protein phosphatase PP1-alpha catalytic subunit	P62137	0.530902765	14	37.54	0.0215679
Ppp2ca	Serine/threonine-protein phosphatase 2A catalytic subunit alpha isoform	P63330	0.61738777	14	35.608	0.0089114
Ppp2r4	Serine/threonine-protein phosphatase 2A activator	P58389;A2AWE9;A2AWF0	0.494359154	9	36.71	0.0280456
Ppp3r1	Calcineurin subunit B type 1;Calcineurin subunit B type 2	Q63810;Q63811	0.301998683	2	19.3	0.0009676
Prdx1	Peroxiredoxin-1	B1AXW5;B1AXW6;P35700;B1AXW4	0.616479021	13	18.87	0.0080862
Prdx2	Peroxiredoxin-2	Q61171;D3Z4A4	0.58665173	6	21.778	0.0220436
Prdx5	Peroxiredoxin-5, mitochondrial	P99029;G3UZJ4;H3BJQ7	0.418471033	10	21.897	0.0051861
Prdx6	Peroxiredoxin-6	D3Z0Y2;Q6GT24;O08709	0.568157463	12	22.494	0.0165047
Prkaca	cAMP-dependent protein kinase catalytic subunit alpha	P05132	0.536532925	14	40.57	0.0222226
Prkacb	cAMP-dependent protein kinase catalytic subunit beta	P68181	0.556321737	12	40.707	0.0115109
Prps1l3	Ribose-phosphate pyrophosphokinase 1	G3UXL2;Q9D7G0;Q8C5R8	0.579861686	10	34.824	0.0162341
Prrc2a	Protein PRRC2A	Q7TSC1;G3UX48	1.906712302	4	229.2	0.016543
Psd3	PH and SEC7 domain-containing protein 3	E9PUC5;Q8C0E9	0.499843469	19	42.299	0.0142997
Psip1	PC4 and SFRS1-interacting protein	Q99JF8;A2BI12	0.608109885	8	59.696	0.002251
Psmb4	Proteasome subunit beta type-4	P99026	0.48362942	5	29.116	5.691E-05
Psmd13	26S proteasome non-ATPase regulatory subunit 13	Q9WVJ2;E9Q5I9;E9Q0 U1	0.523719735	10	42.809	0.0330018
Ptges3	Prostaglandin E synthase 3	D3Z7C6;Q9R0Q7	0.384553575	7	14.982	0.001524
Pura	Transcriptional activator protein Pur-alpha	P42669	0.487308346	7	34.883	0.0031171
Purb	Transcriptional activator protein Pur-beta	O35295	0.556983711	9	33.901	0.0260508
Rab6b	Ras-related protein Rab-6B	P61294	0.62111227	8	23.461	0.0028619
Rabggtb	Geranylgeranyl transferase type-2 subunit beta	Q3TVF4;P53612	0.496553718	2	36.884	0.0294208
Rac1	Ras-related C3 botulinum toxin substrate 1;Ras-related C3 botulinum toxin substrate 2	Q3TLP8;P63001;Q05144	0.526777709	8	23.432	0.0048686
Ran	GTP-binding nuclear protein Ran	P62827;Q14AA6	0.57746916	9	24.423	0.0004582
Rhoa	Transforming protein RhoA;Rho-related GTP-binding protein RhoC	Q9QUI0;A0A0A6YXF6;Q62159	0.527005145	8	21.782	0.0059988
Rhot1	Mitochondrial Rho GTPase 1	Q8BG51	1.490729331	6	72.241	0.0148553
Rnf141	RING finger protein 141	H3BJB4;Q99MB7;H3BK28;H3BJE9; H3BJU0	0.600132262	2	19.846	0.0182967
Rpl17	60S ribosomal protein L17	Q6ZWZ7;Q9CPR4	0.427971634	3	21.397	0.0028499
Rpl22	60S ribosomal protein L22	P67984	0.46220475	3	14.759	0.0114804
Rpl23a	60S ribosomal protein L23a	P62751	0.497281413	5	17.695	0.0289474
Rpl27	60S ribosomal protein L27	P61358	0.51445962	6	15.798	0.0034758
Rpl31	60S ribosomal protein L31	P62900;A0A0A6YXL3;A0A0A6YX26	0.593937441	6	14.463	0.004027
Rps12	40S ribosomal protein S12	Q6ZWZ6;P63323	0.348310303	5	14.515	0.0045595
Rps15a	40S ribosomal protein S15a	F8WJ41;P62245;D3Z712;D3YVB4	0.364219256	6	12.31	0.0013795
Rps17	40S ribosomal protein S17	P63276	0.555238913	3	15.524	0.0221576
Rps18	40S ribosomal protein S18	F6YVP7;P62270;S4R1 N6	0.524654148	9	17.671	0.0324532

(*continued*)

Table 1. (Continued)

Gene name	*Protein name*	*Protein Ac#*	*Female/Male*	*Peptides*	*Mol. weight [kDa]*	p-*value*
Rps19	40S ribosomal protein S19	Q9CZX8;D3YUT3;D3YUG3;D3Z5R8; D3Z722	0.414816094	9	16.085	0.0059377
Rps23	40S ribosomal protein S23	P62267	0.560767596	5	15.807	0.0236718
Rps27a	Ubiquitin-40S ribosomal protein S27a; Ubiquitin;40S ribosomal protein S27a;Ubiquitin-60S ribosomal protein L40;Ubiquitin;60S ribosomal protein L40;Polyubiquitin-B;Ubiquitin;Polyubiquitin-C;Ubiquitin;Ubiquitin-related 1;Ubiquitin-related 2	P62983;A0A0A6YW67;E9Q9J0;E9Q4P0; E9Q5F6;E9QNP0;Q5SX22;P62984; P0CG49;P0CG50;J3QK04;D3YYZ2	0.643132309	6	17.951	0.0060548
Rpsa	40S ribosomal protein SA	P14206	0.53833399	9	32.838	0.0062581
Sae1	SUMO-activating enzyme subunit 1;SUMO-activating enzyme subunit 1, N-terminally processed	Q9R1T2	0.60178259	7	38.62	0.0210271
Sar1a	GTP-binding protein SAR1a	Q99JZ4;P36536	0.562488618	6	22.399	0.0093956
Sbf1	Myotubularin-related protein 5	Q6ZPE2	1.415110365	31	208.69	0.0076232
Sema4a	Semaphorin-4A	D3YWV5;Q62178	2.018920994	3	68.923	0.0284164
Sept7	Septin-7	E9Q1G8;E9Q9F5	0.558382733	23	50.648	0.0048664
Serbp1	Plasminogen activator inhibitor 1 RNA-binding protein	Q9CY58	0.368150136	4	44.714	0.0019796
Serpinb6a	Serpin B6	F8WIV2;Q60854;K7E6F1	0.600940242	8	44.774	0.0154587
Set	Protein SET	A2BE93;Q9EQU5;A2BE92	0.306560856	4	24.923	0.0017287
Sfxn5	Sideroflexin-5;Sideroflexin	Q925 N0;Q8BRQ9	0.526077093	7	37.328	0.0032934
Sgta	Small glutamine-rich tetratricopeptide repeat-containing protein alpha	Q8BJU0	0.565026084	5	34.322	0.0233397
Sh3bgrl	SH3 domain-binding glutamic acid-rich-like protein	Q9JJU8	0.447044935	4	12.811	0.0249732
Sh3bgrl3	SH3 domain-binding glutamic acid-rich-like protein 3	Q91VW3	0.410988452	4	10.477	0.0004383
Sh3gl1	Endophilin-A2	Q62419	0.565981191	12	41.518	0.0001158
Sh3gl2	Endophilin-A1	A2ALV3;Q62420;Q8BXU5;F6ZL13	0.517572539	21	48.295	0.0019956
Sh3gl3	Endophilin-A3	J3QQ44;Q62421;J3QP51;J3QMW2	0.585807068	6	35.098	0.0189954
Shisa6	Protein shisa-6 homolog	Q3UH99;F6VQZ6	2.669986794	2	58.425	0.0427098
Skp1	S-phase kinase-associated protein 1	Q9WTX5	0.376263139	6	18.672	0.0002776
Slc17a6	Vesicular glutamate transporter 2	Q8BLE7	1.605895373	5	64.56	0.0194265
Slc24a2		Q8BUN9;B1AXF2;B1AXF3;F6RT95	1.41229998	6	74.24	0.0054384
Slc2a1	Solute carrier family 2, facilitated glucose transporter member 1	P17809	1.783267586	4	53.984	0.0010345
Slc44a2	Choline transporter-like protein 2	Q8BY89	1.614998084	6	80.109	0.0157501
Slc6a9	Transporter;Sodium- and chloride-dependent glycine transporter 1	E9Q517;E9Q3 V0;P28571	1.92937698	3	58.258	0.0161265
Snca	Alpha-synuclein	O55042	0.426657957	9	14.485	0.0025255
Sncb	Beta-synuclein	Q91ZZ3	0.336865541	6	14.051	0.0016618
Snx3	Sorting nexin-3	Q78ZM0;O70492;D3Z789;D3Z6Z0	0.575986652	7	18.762	0.0012257

(*continued*)

Table 1. (Continued)

Gene name	*Protein name*	*Protein Ac#*	*Female/Male*	*Peptides*	*Mol. weight [kDa]*	p-*value*
Sod1	Superoxide dismutase [Cu-Zn]	P08228	0.370204539	11	15.942	0.002927
Srr	Serine racemase	Q9QZX7	0.56962346	5	36.358	0.0132042
Srrm1	Serine/arginine repetitive matrix protein 1	E9QKA4;A2A8 V8;A2A8 V9;E9PUK6;Q52KI8	2.126989377	3	101.16	0.02442
Srsf1	Serine/arginine-rich splicing factor 1	H7BX95;Q6PDM2	0.532810653	12	28.329	0.0129148
St13	Hsc70-interacting protein	Q99 L47;F8WJK8	0.60498422	10	41.655	0.0046983
Stim2	Stromal interaction molecule 2	I1E4X8;P83093	1.496763123	3	84.77	0.0116701
Stk24	Serine/threonine-protein kinase 24;Serine/threonine-protein kinase 24 35 kDa subunit;Serine/threonine-protein kinase 24 12 kDa subunit;Serine/threonine-protein kinase 26	Q99KH8;A2AD84;Q99JT2	0.629500541	6	47.953	0.0110634
Stmn1	Stathmin	P54227;D3Z5 N2;D3Z1Z8	0.329896735	18	17.274	0.0038518
Stmn2	Stathmin-2	P55821	0.321301263	6	20.828	0.0045284
Strap	Serine-threonine kinase receptor-associated protein	Q9Z1Z2	0.583782213	5	38.442	0.0133315
Stt3a	Dolichyl-diphosphooligosaccharide—protein glycosyltransferase subunit STT3A	P46978	2.087789289	7	80.597	0.0133349
Sv2a	Synaptic vesicle glycoprotein 2A	Q9JIS5	1.567745627	17	82.646	0.0129195
Svop	Synaptic vesicle 2-related protein	Q8BFT9	1.891609321	5	60.768	0.0128867
Synpr	Synaptoporin	D3Z5Q8;Q8BGN8	0.574682292	2	13.719	0.0144322
Syp	Synaptophysin	Q62277	0.556568183	7	34.024	0.0029405
Taldo1	Transaldolase	Q93092	0.558828675	13	37.387	0.0089009
Tbc1d10a	TBC1 domain family member 10A	Q5SPX8;P58802	2.173952831	3	59.195	0.010471
Tbca	Tubulin-specific chaperone A	P48428	0.479415844	2	12.758	0.0006965
Tbcb	Tubulin-folding cofactor B	Q9D1E6	0.601903932	11	27.385	0.0068681
Tceal3	Transcription elongation factor A protein-like 3;Transcription elongation factor A protein-like 5	A2AEC2;Q8R0A5;Q8CCT4;Q9DB24	0.301652187	3	19.925	0.0193945
Tceb1	Transcription elongation factor B polypeptide 1	A0A087WQE6;A0A087WNT1;P83940	0.521323428	3	10.657	0.0304408
Tceb2	Transcription elongation factor B polypeptide 2	P62869	0.429531673	4	13.17	0.0041753
Thnsl1	Threonine synthase-like 1	Q8BH55	1.44080318	5	83.099	0.0082795
Tmod2	Tropomodulin-2	Q9JKK7	0.477825479	14	39.51	0.0114097
Tnr	Tenascin-R	Q8BYI9	1.486284469	32	149.59	0.0104121
Tpi1	Triosephosphate isomerase	P17751;H7BXC3	0.578340921	18	32.191	0.0087338
Tpm1	Tropomyosin alpha-1 chain	G5E8R0;G5E8R1;E9Q455;E9Q453;G5E8R2;E9Q456;E9Q452;Q8BSH3;B7ZNL3;E9Q454;F8WID5;P58771;Q8BP43;E9Q450;E9Q448	0.423636158	17	28.343	0.0075596
Tpm3	Tropomyosin alpha-3 chain	D3Z6I8;E9Q7Q3	0.364830261	25	28.723	0.0066694
Tpm3-rs7	Tropomyosin 3, related sequence 7	D3Z2H9	0.296156924	19	28.991	0.0124408
Trappc10	Trafficking protein particle complex subunit 10	F8VQF9;Q3TLI0	1.628988739	2	141.49	0.0170135
Tsc1	Hamartin	Q9EP53;F2Z3X2	1.68014865	2	128.74	0.0055213
Tsn	Translin	Q62348	0.578560533	6	26.201	0.0120567
Tuba1b	Tubulin alpha-1B chain	P05213	0.650544967	25	50.151	0.0041971

(*continued*)

Table 1. (Continued)

Gene name	*Protein name*	*Protein Ac#*	*Female/Male*	*Peptides*	*Mol. weight [kDa]*	p-*value*
Tubb5	Tubulin beta-5 chain	P99024	0.568695162	23	49.67	0.0011368
Txn	Thioredoxin	P10639	0.168491903	3	11.675	0.0007521
Uba3	NEDD8-activating enzyme E1 catalytic subunit	Q3TL72;Q8C878	0.656410108	3	49.957	0.003456
Ube2d3	Ubiquitin-conjugating enzyme E2 D3; Ubiquitin-conjugating enzyme E2 D2B;Ubiquitin-conjugating enzyme E2 D2	P61079;Q6ZWY6;P62838	0.469795277	2	16.687	4.248E-05
Ube2e3	Ubiquitin-conjugating enzyme E2 E2;Ubiquitin-conjugating enzyme E2 E3;Ubiquitin-conjugating enzyme E2 E1	B2FDH0;D3YW10;D3YXD1;Q91 W82;P52483;H3BKX9;H3BL23; H3BL69;P52482	0.493286163	2	11.116	0.0377247
Ube2k	Ubiquitin-conjugating enzyme E2 K	P61087;D3Z4 U3	0.520291872	4	22.406	0.016896
Ube2l3	Ubiquitin-conjugating enzyme E2 L3	P68037	0.291616217	3	17.861	0.0063496
Ube2m	NEDD8-conjugating enzyme Ubc12	P61082;F6YXS3;F7CDT0;F6WMC0	0.505699639	9	20.9	0.0061667
Ube2n	Ubiquitin-conjugating enzyme E2 N	P61089	0.381017601	10	17.138	0.0012922
Ube2v1	Ubiquitin-conjugating enzyme E2 variant 1	Q9CZY3;B7ZBY7;E9PY39	0.596149877	9	16.355	0.0071458
Ube2v2	Ubiquitin-conjugating enzyme E2 variant 2	Q9D2 M8;A6X925;B2KF55	0.394249227	7	16.367	3.733E-05
Ubfd1	Ubiquitin domain-containing protein UBFD1	Q78JW9	0.35706848	2	40.143	0.0022259
Uchl1	Ubiquitin carboxyl-terminal hydrolase isozyme L1	Q9R0P9	0.367845007	12	24.838	0.0031448
Ufc1	Ubiquitin-fold modifier-conjugating enzyme 1	M0QWS4;Q9CR09	0.53686133	2	11.351	0.0085771
Uqcrb	Cytochrome b-c1 complex subunit 7	Q9CQB4;Q9D855	0.460640217	8	13.561	0.0037272
Usp14	Ubiquitin carboxyl-terminal hydrolase;Ubiquitin carboxyl-terminal hydrolase 14	E9PYI8;Q9JMA1	0.682953821	7	52.318	0.004972
Vbp1	Prefoldin subunit 3	P61759;Q3TIR6	0.495948047	3	22.435	0.0152288
Vps11	Vacuolar protein sorting-associated protein 11 homolog	Q91 W86	1.433046326	5	107.72	0.0024553
Vps29	Vacuolar protein sorting-associated protein 29	D3YYD5;D3Z645;Q9QZ88;D3YW98	0.472022227	4	13.723	0.0100066
Vps41	Vacuolar protein sorting-associated protein 41 homolog	Q5KU39	1.710153771	2	98.601	0.0152951
Vsnl1	Visinin-like protein 1	P62761	0.421303067	9	22.142	0.0015797
Wbp2	WW domain-binding protein 2	A2A860;P97765	0.49979446	6	23.308	0.0015928
Wdr46	WD repeat-containing protein 46	Q9Z0H1	1.410146605	2	69.047	0.0078564
Ykt6	Synaptobrevin homolog YKT6	Q9CQW1	0.486076475	8	22.314	0.0158255
Ywhab	14-3-3 protein beta/alpha;14-3-3 protein beta/alpha, N-terminally processed	Q9CQV8;A2A5 N1	0.472609405	13	28.086	0.0101889
Ywhae	14-3-3 protein epsilon	P62259;D6REF3;F6WA09	0.561506617	19	29.174	0.0110828
Ywhag	14-3-3 protein gamma;14-3-3 protein gamma, N-terminally processed	P61982	0.578935838	16	28.302	0.0081541
Ywhah	14-3-3 protein eta	P68510	0.495943458	16	28.211	0.0027942
Ywhaq	14-3-3 protein theta	F6VW30;P68254;F6YY69	0.638659652	14	34.348	0.0174277
Ywhaz	14-3-3 protein zeta/delta	P63101	0.543366191	16	27.771	0.0158234

TABLE 2. LIST OF PHOSPHOSITES DIFFERENTIALLY PHOSPHORYLATED IN FEMALE VERSUS MALE LEFT AUDITORY CORTEX AFTER OXYTOCIN INFUSION

Gene name	*Protein name*	*Protein Ac.#*	*Female/ Male*	*Modified sequence*	*Phosphorylated amino acid*	p- *value*
Limch1	LIM and calponin homology domains-containing protein 1	D3YV55	2.938025187	GSSDGRGS(ph)DSESDLPHR	Serine 75	0.000387
Ttbk1	Tau-tubulin kinase 1	Q6PCN3	2.895142788	RVNS(ph)PESER	Serine 456	0.000578
Cltc	Clathrin heavy chain 1	Q5SXR6	2.827696169	GILRT(ph)PDTIR	Threonine 398	0.003383
Cul9	Cullin-9	E9QP09	1.559321501	ELGS(ph)LPSSR	Serine 584	0.0002
Kifap3	Kinesin-associated protein 3	P70188	0.542152187	RDS(ph)LPGK	Serine 102	0.000748
Camk2b	Calcium/calmodulin-dependent protein kinase type II subunit beta	Q5SVI0	0.421062607	NSSAITS(ph)PK	Serine 343	1.44E-05
Ncam1	Neural cell adhesion molecule 1	A0A0A6YY91	0.298598535	NPPEAATAPAS(ph)PK	Serine 979	0.004037
Ccsap	Centriole, cilia, and spindle-associated protein	Q8QZT2	0.294310064	AHS(ph)VDVEK	Serine 222	0.000375

closely matching the time course of retrieval behavior onset (Fig. 4b). Males cannot nurse pups, but another important difference we noticed between cohoused males and females is that the dams and cohoused male mice quickly mated soon after cohousing began. Mating may provide important contributions to the onset of male parenting behaviors, even when these behaviors are first expressed considerably later in time after mating as previously described by Wu *et al.*[44]

After days of cohousing, retrieval behavior was expressed similarly in males and saline-injected females. The major effect of oxytocin was to accelerate this process in female cohoused virgins (Fig. 4c), with no effect in males. Saline-injected females began expressing retrieval slightly earlier than males; after 24 h of cohousing, the number of females retrieving was double that of males (Fig. 4d, ''1 day''). However, after a week, these fractions were equivalent, with about half of all males and saline-injected females retrieving (Fig. 4d, ''7 days''). Thus male mice can express parental behaviors in a similar manner as females, although some females can express these behaviors with less maternal experience, as well as remain sensitive to oxytocin supplements that increase and accelerate the rate of behavioral expression.

Discussion

In this study we examined the expression patterns and functions of oxytocin receptors in mouse auditory cortex. We showed that adult female mouse left auditory cortex has more cells expressing oxytocin receptors than male cortex or female right auditory cortex. Previously we observed in female mouse auditory cortex that the relative number of OXTR-2^+ cells increased from the first to the second postnatal week in both left and right hemispheres, but then decreased from postnatal week 2 to adulthood, decreasing more in right female auditory cortex than left auditory cortex.[21] In other words, receptor levels were initially at a moderate level in early postnatal females and males, peaked during the second postnatal week, and declined to an equivalent degree in males and female right auditory cortex, leaving receptor expression levels higher in female left auditory cortex.

This is consistent with the cortical developmental profile of receptor expression first described by Hammock and Levitt,[59] with the additional finding of the hemispheric differences in females. As we reported in this study, OXTR-2 labeling was similarly high in postnatal week 2 males and females, but decreased to adult levels in parallel with a reduction in oxytocin receptor mRNA levels. These adult levels are therefore less decreased in female left auditory cortex compared to female right or male auditory cortex of either hemisphere. This was the sole identifiable difference between males and females in terms of peptide modulation of central auditory system structures examined here, with little oxytocin receptor expression or mRNA in adult auditory thalamus, and virtually no detectable vasopressin V1a receptor mRNA in either cortex or thalamus of older mice.

The specific pattern of receptor expression should confer certain properties on oxytocin signaling in the mammalian brain. Previous reports of the distributions of oxytocin receptors have relied on autoradiography or *in situ* hybridization.[5–7,23,24,26] These studies have been important for

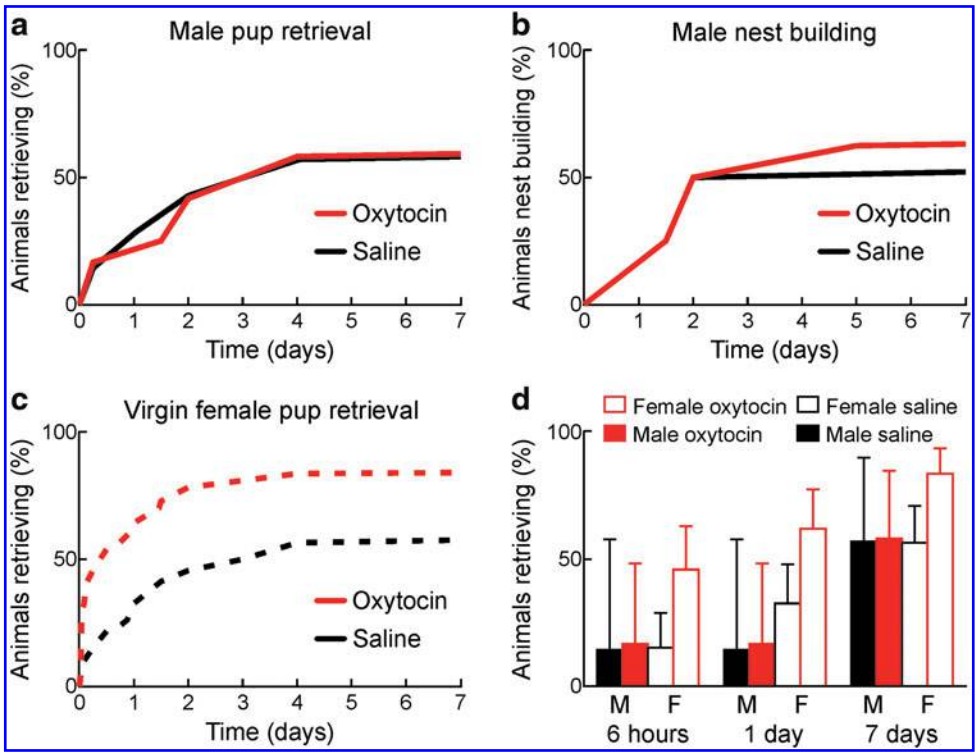

FIG. 4. Oxytocin does not accelerate onset of parental behaviors in male C57BL/6 mice. **(a)** Cumulative percentage of initially-naive males retrieving starting after cohousing on day 0, receiving saline injections (*black*, $N=7$) or oxytocin (*red*, $N=12$). Oxytocin-injected males did not retrieve faster or at higher levels overall than saline-injected males. **(b)** Cumulative percentage of males expressing nest building behavior after cohousing starting on day 0. Oxytocin- and saline-injected males began to build nests at similar rates; same male mice as in **(a)**. **(c)** Cumulative percentage of initially-naive virgin females retrieving starting after cohousing on day 0, receiving saline injections (*black*, $N=46$) or oxytocin (*red*, $N=37$). Oxytocin accelerated retrieval onset and increased number of animals retrieving overall. **(d)** Summary of pup retrieval by cohoused mice (*filled bars*) and female (*open bars*) mice receiving either saline (*black*) or oxytocin (*red*) injections, at 6 h after cohousing (saline injected: 1/7 males retrieving, 7/46 females retrieving, $p=0.99$ with two-tailed Fisher's exact test; oxytocin injected: 2/12 males retrieving, 17/37 females retrieving, $p=0.095$); 1 day after cohousing (saline injected: 1/7 males retrieving, 15/46 females retrieving, $p=0.411$; oxytocin injected: 2/12 males retrieving, 23/37 females retrieving, $p=0.008$); and 7 days after cohousing (saline injected: 4/7 males retrieving, 26/46 females retrieving, $p=0.99$; oxytocin injected: 7/12 males retrieving, 31/37 females retrieving, $p=0.108$). Statistics and error bars are mean ± 95% confidence intervals.

determining which brain structures express oxytocin receptors. Recently we developed the OXTR-2 antibodies used in this study and found in female left auditory cortex that the majority of cells expressing oxytocin receptors were cortical inhibitory interneurons,[18,21] similar to a study in transgenic animals demonstrating oxytocin receptors in somatostatin interneurons of mouse prefrontal cortex.[30]

This agrees with the functional effects of oxytocin receptor activation for modulating synaptic transmission. Specifically, in adult auditory cortex, olfactory piriform cortex, PVN, and hippocampal CA1, oxytocin has been found to reduce GABAergic transmission.[18,21,62] This disinhibition of principal cells in each area leads to increased excitability, promotes LTP induction, and in PVN might underlie the phenomenon of oxytocin-induced oxytocin release.[6,18,21,63] In the central auditory system, auditory cortical neurons in experienced maternal animals but not pup-naive animals can reliably respond to pup call sounds,[18,64–66] and activity in the left but not right auditory cortex is required for experienced mother mice to respond to infant distress sounds for pup retrieval.[18,67] In naive female auditory cortex, the reduction of inhibition produced by oxytocin should make the cortical network much more responsive to incoming inputs such as pup calls that co-occur with heightened periods of oxytocin release. Repetitive presentation of the sensory signals in the disinhibited state would then induce enduring representational plasticity for pup cues[18] through mechanisms of NMDA-receptor-dependent LTP,[21] making maternal recognition of pup distress much more rapid and reliable. We speculate that the extensive amount of protein regulation and phosphorylation observed in this study in the left auditory cortex after oxytocin treatment might be related to expression of long-term synaptic modifications. The functional effects and interrelations between these genes will require further investigation, particularly in terms of lateralization in the female cortex.

We hypothesize that the left lateralization of oxytocin receptor expression in female auditory cortex confers a selective advantage for recognizing conspecific vocalizations, especially infant distress calls. This might manifest as circuit-level specializations on the left (and possibly right) hemispheres, consistent with hemispheric parcellation of

specific auditory functions in human left versus right temporal lobes from imaging studies[68] (Hickok and Poeppel 2007). A left-lateralized preference for underlying pup call modulation rhythms might also lead to selectivity for or perceptual categorization of pup calls in the left auditory cortex presented at the natural call rates ($\sim$3–8 Hz); this would only be the case if this pup call rhythm or bout rate was the predominant acoustic feature used by experienced co-carers for recognizing distress calls, as opposed to strictly their component ultrasonic frequencies. Furthermore, asymmetries in inhibitory neuron circuit composition might convey differential temporal sensitivities to the left and right sides; we note that most oxytocin receptors are expressed on cortical interneurons and regulate GABAergic transmission.[18,21,30,62] Oxytocin receptor activation in left auditory cortex might lead directly to changes in protein expression and phosphorylation through mechanisms downstream of G protein-coupled receptor signaling or indirectly lead to changes in activity-dependent gene regulation after increased excitability or LTP induction.

Why might oxytocin enhance retrieval onset in females but not males? Additionally or instead, it is also possible that other factors contribute to this sex specificity of oxytocin action. First, oxytocin may have little to do with emergence of paternal behavior in males. For example, pair bonding in adult voles displays a similar sex-specific enhancement by oxytocin supplements. Exogenous oxytocin was found to increase pair bonding in females but had little effect in males, which might instead be regulated by vasopressin.[69] In male C57BL/6 mice, galanin neurons might be more important for initiating these behaviors after cohousing and mating.[44]

Second, native release of endogenous oxytocin during or after social interactions and mating might be higher or lead to saturating activation of oxytocin receptors in males, but occur at more moderate levels in females.[70] However, measurement of endogenous oxytocin in amygdala during social interest behavior revealed similar peptide levels in male and female rats, indicating that central release of the hormone may not play a major role in sex-specific differences to oxytocin modulation.[71]

Third, blood–brain barrier permeability could be more permissive in females than males,[72] enabling systemic oxytocin to have more access to the female central nervous system. Finally, peripheral treatment with oxytocin might bind to peripheral oxytocin receptors, which are expressed by many tissues and cell types outside of the brain.[6] Activation of peripheral receptors might indirectly affect central activity, perhaps further stimulating endogenous oxytocin release to enhance parental behavior.[63,73] Little is known about the potential for these processes to provide mechanisms for oxytocin signaling throughout the organism, and it remains unclear how peripheral oxytocin administration affects neural activity to influence social cognition in any mammalian species.

Sex-specific differences in regional oxytocin receptor expression are consistent with the major role of this hormone in maternal physiology. In rat forebrain, Dumais *et al.*[74] found that most brain areas examined had lower oxytocin receptor radiolabel binding in females than in males. These regions included ventromedial hypothalamus (VMH), hippocampal CA1, the medial preoptic area (MPOA), nucleus accumbens, the bed nucleus of the stria terminalis (BNST), and medial amygdala. In agreement, our characterization of oxytocin receptor expression with OXTR-2 labeling[21] revealed that many of these same areas had higher expression levels in female mice (dams or virgins) than in males, consistent with these areas serving as a distributed network regulated by oxytocin, likely important for social and maternal behavior. One interesting difference is that while estrus led to higher oxytocin receptor radiolabel binding densities in female rats in most subcortical areas examined (including MPOA, VMH, BNST, and nucleus accumbens),[5,74] we found that estrus did not affect oxytocin receptor expression in female mouse auditory cortex.[21] Regional differences in oxytocin receptor expression and regulation of receptor levels during estrus are believed to be due, in part, to a hormone response element upstream from the oxytocin receptor transcription initiation site.[10] This suggests that perhaps during postnatal development or puberty, steroid hormone signaling helps pattern receptor expression across different brain areas and in a sex-specific manner; such a mechanism might also be important for emergence of left-lateralized oxytocin receptor expression during postnatal development in female mice.

More studies are also required to understand the cellular mechanisms and functional significance of oxytocin receptor lateralization in female auditory cortex. In general, it is unknown how larger scale neural organizational features (such as retinotopy in the visual system or tonotopy in the auditory system) relate to the functions of those systems, although it seems reasonable to expect that such organization might improve detection and recognition of important sensory signals such as pup distress calls, by clustering cells together to ensure a more coherent network-level response from cells with similar robust tuning properties.[75,76] Given the sparseness of axonal projections from hypothalamic oxytocin neurons throughout the brain,[6,12,18,21] enhanced density of cells expressing oxytocin receptors, located together in a local cluster, might also facilitate oxytocin modulation especially if this system relies on volume transmission. Finally, left-lateralized oxytocin receptor expression in female auditory cortex is reminiscent of some features of human speech and language representation.[68,77,78] Understanding the mechanisms and consequences of asymmetrical cortical pup call processing might therefore provide some information about the biological basis of human language abilities.

Conclusion

Female and male mice both can express parental behaviors such as pup retrieval within hours to days after initial contact with pups and experienced mothers. Females naturally exhibited maternal behaviors somewhat earlier than males, and exogenous oxytocin augmented the speed and relative number of females but not males displaying parental behaviors. As the only apparent difference between oxytocin receptor expression in adult males and females was a higher level of receptor expression in female left auditory cortex, we suggest that this left lateralization might provide a biological basis for oxytocin to enhance maternal behavior.

Acknowledgments

This work was funded by NICHD (HD088411 to R.C.F.), NIDCD (DC009635 and DC012557 to R.C.F., DC012527

and DC015388 to T.A.H.), NINDS (NS21072 to M.V.C.; T32 NS086750 fellowship to M.M.), NIMH (T32 MH019524 fellowship to B.J.M.), a McKnight Scholarship (R.C.F.), a Pew Scholarship (R.C.F.), a Sloan Research Fellowship (R.C.F.), a Howard Hughes Medical Institute Faculty Scholarship (R.C.F.), and a Skirball Institute Collaborative Research Award (M.V.C. and R.C.F.). The authors thank I. Carcea, M. Jin, N. Lopez, E. Xh. Morina, and N. Zaika for comments, discussions, and technical assistance and C.A. Loomis and the NYU School of Medicine Histology Core for assistance with anatomical studies.

Author Disclosure Statement

No conflicts of interest exist.

References

1. Bloom FE. Neuropeptides. Sci Am 1981;245:148–168.
2. Insel TR, Young LJ. The neurobiology of attachment. Nat Rev Neurosci 2001;2:129–136.
3. Dulac C, O'Connell LA, Wu Z. Neural control of maternal and paternal behaviors. Science 2014;345:765–770.
4. Rilling JK, Young LJ. The biology of mammalian parenting and its effects on offspring social development. Science 2014;345:771–776.
5. Dumais KM, Veenema AH. Vasopressin and oxytocin receptor systems in the brain: sex differences and sex-specific regulation of social behavior. Front Neuroendocrinol 2016; 40:1–23.
6. Froemke RC, Carcea I. Oxytocin and brain plasticity. In: Legato MJ, ed. Principles of gender-specific medicine. 3rd ed. Cambridge, MA: Academic Press; 2017. p. 161–182.
7. Vaidyanathan R, Hammock EA. Oxytocin receptor dynamics in the brain across development and species. Dev Neurobiol 2017;77:143–157.
8. Rhodes CH, Morrell JI, Pfaff DW. Immunohistochemical analysis of magnocellular elements in rat hypothalamus: distribution and numbers of cells containing neurophysin, oxytocin, and vasopressin. J Comp Neurol 1981;198:45–64.
9. Swanson LW, Sawchenko PE. Hypothalamic integration: organization of the paraventricular and supraoptic nuclei. Annu Rev Neurosci 1983;6:269–324.
10. Gimpl G, Fahrenholz F. The oxytocin receptor system: structure, function, and regulation. Physiol Rev 2001;81: 629–683.
11. Wakerley JB. Milk ejection and its control. In: Niell J, ed. Knobil and Neill's physiology of reproduction, 3rd ed. Amsterdam, The Netherlands: Elsevier; 2006. p. 3129–3190.
12. Dölen G. Oxytocin: parallel processing in the social brain? J Neuroendocrinol 2015;27:516–535.
13. Elands J, Beetsma A, Barberis C, et al. Topography of the oxytocin receptor system in rat brain: an autoradiographical study with a selective radioiodinated oxytocin antagonist. J Chem Neuroanat 1988;1:293–302.
14. Richard P, Moos F, Freund-Mercier MJ. Central effects of oxytocin. Physiol Rev 1991;71:331–370.
15. Cui Z, Gerfen CR, Young WS. Hypothalamic and other connections with dorsal CA2 area of the mouse hippocampus. J Comp Neurol 2013;521:1844–1866.
16. Dölen G, Darvishzadeh A, Huang KW, et al. Social reward requires coordinated activity of nucleus accumbens oxytocin and serotonin. Nature 2013;501:179–184.
17. Zheng JJ, Li SJ, Zhang XD, et al. Oxytocin mediates early experience dependent cross-modal plasticity in the sensory cortices. Nat Neurosci 2014;17:391–399.
18. Marlin BJ, Mitre M, D'amour JA, et al. Oxytocin enables maternal behaviour by balancing cortical inhibition. Nature 2015;520:499–504.
19. Scott N, Prigge M, Yizhar O, et al. A sexually dimorphic hypothalamic circuit controls maternal care and oxytocin secretion. Nature 2015;525:519–522.
20. Grinevich V, Knobloch-Bollmann HS, Eliava M, et al. Assembling the puzzle: pathways of oxytocin signaling in the brain. Biol Psychiatry 2016;79:155–164.
21. Mitre M, Marlin BJ, Schiavo JK, et al. A distributed network for social cognition enriched for oxytocin receptors. J Neurosci 2016;36:2517–2535.
22. Pedersen CA, Ascher JA, Monroe YL, et al. Oxytocin induces maternal behavior in virgin female rats. Science 1982;216:648–650.
23. Tribollet E, Charpak S, Schmidt A, et al. Appearance and transient expression of oxytocin receptors in fetal, infant, and peripubertal rat brain studied by autoradiography and electrophysiology. J Neurosci 1989;9:1764–1773.
24. Insel T. Regional changes in brain oxytocin receptors postpartum: time-course and relationship to maternal behaviour. J Neuroendocrinol 1990;2:539–545.
25. McCarthy MM. Oxytocin inhibits infanticide in female house mice (Mus domesticus). Horm Behav 1990;24:365–375.
26. Insel TR, Shapiro LE. Oxytocin receptor distribution reflects social organization in monogamous and polygamous voles. Proc Natl Acad Sci U S A 1992;89:5981–5985.
27. Nishimori K, Young LJ, Guo Q, et al. Oxytocin is required for nursing but is not essential for parturition or reproductive behavior. Proc Natl Acad Sci U S A 1996;93: 11699–11704.
28. Olazábal DE, Young LJ. Oxytocin receptors in the nucleus accumbens facilitate ''spontaneous'' maternal behavior in adult female prairie voles. Neuroscience 2006;141:559–568.
29. Wacker DW, Ludiwig M. Vasopressin, oxytocin, and social odor recognition. Horm Behav 2012;61:259–265.
30. Nakajima M, Görlich A, Heintz N. Oxytocin modulates female sociosexual behavior through a specific class of prefrontal cortical interneurons. Cell 2014;159:295–305.
31. Jiménez A, Young LJ, Río RTD, et al. Neuroanatomical distribution of oxytocin receptor binding in the female rabbit forebrain: variations across the reproductive cycle. Brain Res 2015;1629:329–339.
32. Chini B, Verhage M, Grinevich V. The action radius of oxytocin release in the mammalian CNS: from single vesicles to behavior. Trends Pharmacol Sci 2017;38:982–991.
33. Andari E, Duhamel JR, Zalla T, et al. Promoting social behavior with oxytocin in high-functioning autism spectrum disorders. Proc Natl Acad Sci U S A 2010;107:4389–4394.
34. Bartz JA, Zaki J, Bolger N, et al. Social effects of oxytocin in humans: context and person matter. Trends Cogn Sci 2011;15:301–309.
35. Churchland PS, Winkielman P. Modulating social behavior with oxytocin: how does it work? What does it mean? Horm Behav 2012;61:392–399.
36. Peñagarikano O, Lázaro MT, Lu XH, et al. Exogenous and evoked oxytocin restores social behavior in the Cntnap2 mouse model of autism. Sci Transl Med 2015;7:27.

37. Walum H, Waldman ID, Young LJ. Statistical and methodological considerations for the interpretation of intranasal oxytocin studies. Biol Psychiatr 2016;79:251–257.
38. Kendrick KM, Guastella AJ, Becker B. Overview of human oxytocin research. Curr Top Behav Neurosci 2017 [Epub ahead of print]; DOI: 10.1007/7854_2017_19.
39. Gubernick DJ, Alberts JR. Postpartum maintenance of paternal behaviour in the biparental California mouse, Peromyscus californicus. Anim Behav 1989;37:656–664.
40. Bester-Meredith JK, Marler CA. Vasopressin and the transmission of paternal behavior across generations in mated, cross-fostered Peromyscus mice. Behav Neurosci 2003;117:455–463.
41. Wynne-Edwards KE, Timonin ME. Paternal care in rodents: weakening support for hormonal regulation of the transition to behavioral fatherhood in rodent animal models of biparental care. Horm Behav 2007;52:114–121.
42. Carter CS, Boone EM, Pournajafi-Nazarloo H, et al. Consequences of early experiences and exposure to oxytocin and vasopressin are sexually dimorphic. Dev Neurosci 2009;31:332–341.
43. Liu HX, Lopatina O, Higashida C, et al. Displays of paternal mouse pup retrieval following communicative interaction with maternal mates. Nat Commun 2013;4: 1346.
44. Wu Z, Autry AE, Bergan JF, et al. Galanin neurons in the medial preoptic area govern parental behaviour. Nature 2014;509:325–330.
45. Akther S, Huang Z, Liang M, et al. Paternal retrieval behavior regulated by brain estrogen synthetase (Aromatase) in mouse sires that engage in communicative interactions with pairmates. Front Neurosci 2015;9:450.
46. Chary MC, Cruz JP, Bardi M, et al. Paternal retrievals increase testosterone levels in both male and female California mouse (Peromyscus californicus) offspring. Horm Behav 2015;73:23–29.
47. Bendesky A, Kwon YM, Lassance JM, et al. The genetic basis of parental care evolution in monogamous mice. Nature 2017;544:434–439.
48. Amico JA, Tenicela R, Johnston J, et al. A time-dependent peak of oxytocin exists in cerebrospinal fluid but not in plasma of humans. J Clin Endocrinol Metab 1983;57:947–951.
49. Gubernick DJ, Winslow JT, Jensen P, et al. Oxytocin changes in males over the reproductive cycle in the monogamous, biparental California mouse, Peromyscus californicus. Horm Behav 1995;29:59–73.
50. Schneiderman I, Zagoory-Sharon O, Leckman JF, et al. Oxytocin during the initial stages of romantic attachment: relations to couples' interactive reciprocity. Psychoneuroendocrinology 2012;37:1277–1285.
51. Hinde K, Muth C, Maninger N, et al. Challenges to the pair bond: neural and hormonal effects of separation and reunion in a monogamous primate. Front Behav Neurosci 2016;10:221.
52. Olazábal DE, Alsina-Llanes M. Are age and sex differences in brain oxytocin receptors related to maternal and infanticidal behavior in naïve mice? Horm Behav 2016;77: 132–140.
53. Hackett TA, Clause AR, Takahata T, et al. Differential maturation of vesicular glutamate and GABA transporter expression in the mouse auditory forebrain during the first weeks of hearing. Brain Struct Funct 2015;16:606.
54. Huang FK, Zhang GA, Lawlor K, et al. Deep coverage of global protein expression and phosphorylation in breast tumor cell lines using TMT 10-plex isobaric labeling. J Proteome Res 2017;16:1121–1132.
55. Rappsilber J, Mann M, Ishihama Y. Protocol for micropurification, enrichment, pre-fractionation and storage of peptides for proteomics using StageTips. Nat Protocols 2007;2:1896–1906.
56. Cox J, Neuhauser N, Michalski A, et al. Andromeda: a peptide search engine integrated into the MaxQuant environment. J Proteome Res 2011;10:1794–1805.
57. Tyanova S, Temu T, Cox J. The MaxQuant computational platform for mass spectrometry-based shotgun proteomics. Nat Protocols 2016;11:2301–2319.
58. Ritchie ME, Phipson B, Wu D, et al. Limma powers differential expression analyses for RNA-sequencing and microarray studies. Nucleic Acids Res 2015;43:e47.
59. Hammock EA, Levitt P. Oxytocin receptor ligand binding in embryonic tissue and postnatal brain development of the C57BL/6J mouse. Front Behav Neurosci 2013;7:195.
60. Maier T, Güell M, Serrano L. Correlation of mRNA and protein in complex biological samples. FEBS Lett 2009; 583:3966–3973.
61. Vogel C, Marcotte EM. Insights into the regulation of protein abundance from proteomic and transcriptomic analyses. Nat Rev Genet 2012;13:227–232.
62. Owen SF, Tuncdemir SN, Bader PL, et al. Oxytocin enhances hippocampal spike transmission by modulating fast-spiking interneurons. Nature 2013;500:458–462.
63. Moos F, Freund-Mercier MJ, Guerné Y, et al. Release of oxytocin and vasopressin by magnocellular nuclei in vitro: specific facilitatory effect of oxytocin on its own release. J Endocrinol 1984;102:63–72.
64. Ehret G. Infant rodent ultrasounds—a gate to the understanding of sound communication. Behav Genet 2005;35: 19–29.
65. Liu RC, Schreiner CE. Auditory cortical detection and discrimination correlates with communicative significance. PLoS Biol 2007;5:e173.
66. Cohen L, Rothschild G, Mizrahi A. Multisensory integration of natural odors and sounds in the auditory cortex. Neuron 2011;72:357–369.
67. Ehret G. Left hemisphere advantage in the mouse brain for recognizing ultrasonic communication calls. Nature 1987; 325:249–251.
68. Hickok G, Poeppel D. The cortical organization of speech processing. Nat Rev Neurosci 2007;8:393–402.
69. Insel TR, Hulihan TJ. A gender-specific mechanism for pair bonding: oxytocin and partner preference formation in monogamous voles. Behav Neurosci 1995;109:782–789.
70. Sano Y, Watanabe N, Suzuki E, et al. A cohort study of the level of plasma oxytocin associated with autism spectrum disorder in Japanese males, females and pregnant females. Clin Med Biochem 2016;2:113.
71. Dumais KM, Alonso AG, Bredewold R, et al. Role of the oxytocin system in amygdala subregions in the regulation of social interest in male and female rats. Neuroscience 2016;330:138–149.
72. Oztaş B, Koçak H, Oner P, et al. Sex-dependent changes in blood-brain barrier permeability and brain NA(+),K(+) ATPase activity in rats following acute water intoxication. J Neurosci Res 2000;62:750–753.
73. Welch MG, Tamir H, Gross KJ, et al. Expression and developmental regulation of oxytocin (OT) and oxytocin receptors (OTR) in the enteric nervous system (ENS) and intestinal epithelium. J Comp Neurol 2009;512:256–270.

74. Dumais KM, Bredewold R, Mayer TE, et al. Sex differences in oxytocin receptor binding in forebrain regions: correlations with social interest in brain region- and sex-specific ways. Horm Behav 2013;64:693–701.
75. Knudsen EI, du Lac S, Esterly SD. Computational maps in the brain. Annu Rev Neurosci 1987;10:41–65.
76. Chklovskii DB, Koulakov AA. Maps in the brain: what can we learn from them? Annu Rev Neurosci 2004;27:369–392.
77. Loring DW, Meador KJ, Lee GP, et al. Cerebral language lateralization: evidence from intracarotid amobarbital testing. Neuropsychologia 1990;28:831–838.
78. Bishop DV. Cerebral asymmetry and language development: cause, correlate, or consequence? Science 2013;340: 1230531.

Address correspondence to:
Robert C. Froemke, PhD
Skirball Institute 5–9
Departments of Otolaryngology,
Neuroscience and Physiology
NYU School of Medicine
540 First Avenue
New York, NY 10016

E-mail: robert.froemke@med.nyu.edu

Received for publication September 27, 2017; received in revised form November 7, 2017; accepted November 9, 2017.